© 2021. Published by The Company of Biologists Ltd | Journal of Cell Science (2021) 134, jcs258769. doi:10.1242/jcs.258769

RESEARCH ARTICLE

Protein tyrosine phosphatase 1B targets focal adhesion kinase and paxillin in cell–matrix adhesions

Ana E. González Wusener[1,*], Ángela González[1,*], María E. Perez Collado[1], Melina R. Maza[2], Ignacio J. General[2] and Carlos O. Arregui[1,‡]

ABSTRACT

Protein tyrosine phosphatase 1B (PTP1B, also known as PTPN1) is an established regulator of cell-matrix adhesion and motility. However, the nature of substrate targets at adhesion sites remains to be validated. Here, we used bimolecular fluorescence complementation assays, in combination with a substrate trapping mutant of PTP1B, to directly examine whether relevant phosphotyrosines on paxillin and focal adhesion kinase (FAK, also known as PTK2) are substrates of the phosphatase in the context of cell-matrix adhesion sites. We found that the formation of catalytic complexes at cell-matrix adhesions requires intact tyrosine residues Y31 and Y118 on paxillin, and the localization of FAK at adhesion sites. Additionally, we found that PTP1B specifically targets Y925 on the focal adhesion targeting (FAT) domain of FAK at adhesion sites. Electrostatic analysis indicated that dephosphorylation of this residue promotes the closed conformation of the FAT 4-helix bundle and its interaction with paxillin at adhesion sites.

KEY WORDS: PTP1B, Paxillin, FAK, BiFC, Adhesions

INTRODUCTION

Specialized adhesion complexes in the plasma membrane transduce chemical and physical properties of the extracellular matrix in intracellular signaling that regulates different aspects of cell behavior, including motility, survival and proliferation (Giancotti and Ruoslahti, 1999; Miranti and Brugge, 2002; Ringer et al., 2017). To obtain a full understanding of the molecular mechanisms implied in signal transduction it is necessary to identify the components of cell-matrix adhesion complexes (‘adhesome’), as well as being aware of their functional spatiotemporal relationships. Post-translational modifications of proteins make this last task challenging, especially when some of these modifying processes, such as phosphorylation, are transient and highly encoded in space and time (Ballestrem et al., 2006; Kholodenko et al., 2010; Zaidel-Bar and Geiger, 2010).

Focal adhesion kinase (FAK, also known as PTK2) and Src family kinases play a prominent role in the phosphorylation of adhesome components (Byron et al., 2015; Horton et al., 2016; Robertson et al., 2015; Volberg et al., 2001). Conspicuous substrates include the adaptor proteins paxillin and p130Cas (also known as BCAR1), as well as the FAK and Src kinases themselves (Ballestrem et al., 2006; González Wusener et al., 2016; Mitra and Schlaepfer, 2006; Xie et al., 2016). FAK is autophosphorylated on tyrosine (Tyr) 397 in the FERM-kinase linker, an event that generates a binding site for the Src SH2 domain (Schaller et al., 1994). Src phosphorylates and regulates different tyrosines and outputs on FAK (Martínez et al., 2020; Walkiewicz et al., 2015). Phosphorylation of FAK tyrosines 576 and 577 in the activation loop promotes maximal FAK activity (Calalb et al., 1995; Lietha et al., 2007), and phosphorylation of Tyr-925 at the C-terminal focal adhesion targeting (FAT) domain promotes interaction with Grb2 and the activation of Erk2 (also known as MAPK1) (Brunton et al., 2005; Schlaepfer and Hunter, 1996a; Schlaepfer et al., 1994). Structural studies suggest that the FAT domain exists in two conformation states: as a compact four-helix bundle, and in an ‘open’ conformation in which helix1 is separated from the helix bundle. In the open conformation, Tyr-925 is exposed and more susceptible to phosphorylation and interaction with the SH2 domain of Grb2, while inhibiting the interaction with paxillin. In contrast, the compact conformation interacts with leucine-aspartic acid (LD) motifs 2 and 4 of paxillin, and excludes the phosphorylation of Tyr-925 and Grb2 binding (Arold et al., 2002; Deramaudt et al., 2011; Hayashi et al., 2002; Hoellerer et al., 2003; Kadaré et al., 2015; Liu et al., 2002; Prutzman et al., 2004). Thus, the phosphorylation state of Tyr-925 at the FAT domain may function as a switch leading to different FAK outputs.

In response to cell adhesion, FAK and Src phosphorylate tyrosines 31 and 118 on paxillin (Bellis et al., 1995; Schaller and Parsons, 1995), generating binding sites for the SH2 domains of Crk, Csk and p120RasGAP (also known as RASA1), and promoting cell motility (Petit et al., 2000; Schaller and Parsons, 1995; Tsubouchi et al., 2002). Paxillin tyrosine phosphorylation also enhances the association with FAK and vinculin through unknown mechanisms (Case et al., 2015; Choi et al., 2011; Pasapera et al., 2010; Zaidel-Bar et al., 2007).

Super-resolution analysis of cell-matrix adhesion complexes revealed a multilaminar organization of their components (Braniš et al., 2017; Case et al., 2015; Kanchanawong et al., 2010). A layer juxtaposed to the plasma membrane contains, in addition to integrin cytoplasmic tails, regulators of integrin activation and initiators of signaling (signaling layer), including talin 1, FAK and paxillin. A deeper layer includes proteins playing a mechanotransduction role, such as vinculin, talin 1, and p130Cas, among others. Components of this layer also contribute to form the physical bridge between integrin tails and the most interior strata composed of actin regulatory proteins and actin filaments. Several protein tyrosine phosphatases were identified in the proteomic analysis of cell-matrix adhesions, including the endoplasmic reticulum (ER)-bound PTP1B (also known as PTPN1; Byron et al., 2015; Robertson et al., 2015; Zaidel-Bar et al., 2007).

[1]Instituto de Investigaciones Biotecnológicas, Universidad Nacional de San Martín and Consejo Nacional de Investigaciones Científicas y Técnicas (CONICET), San Martín, Buenos Aires 1650, Argentina. [2]Escuela de Ciencia y Tecnología, Universidad Nacional de San Martin, Instituto de Ciencias Físicas and CONICET, San Martin, Buenos Aires 1650, Argentina.
*These authors contributed equally to this work

‡Author for correspondence (carregui@iib.unsam.edu.ar)

C.O.A., 0000-0003-0704-3321

Handling Editor: Arnoud Sonnenberg
Received 12 April 2021; Accepted 14 September 2021

Journal of Cell Science (2021) 134, jcs258769. doi:10.1242/jcs.258769

Work from several groups, including ours, suggests a regulatory role for PTP1B in cell-matrix adhesion (Arias-Salgado et al., 2005; Arregui et al., 1998, 2013; Burridge et al., 2006; Byron et al., 2015; Cheng et al., 2001; Liu et al., 1998; Pradhan et al., 2010; Robertson et al., 2015; Zaidel-Bar et al., 2007). We have previously shown that immortalized PTP1B knockout fibroblasts display several alterations of cell-matrix adhesions and migration, including defective adhesion maturation and unstable protrusions (Burdisso et al., 2013; Hernández et al., 2006). In agreement with the high spatial correlation and coupled dynamics between the ER and microtubules at the cell periphery revealed by time-lapse studies (Waterman-Storer and Salmon, 1998), we have shown that ER-bound PTP1B-GFP is positioned near the plasma membrane and bound to the substratum in a microtubule-dependent manner and establishes complexes with Src and α-actinin 1 (Burdisso et al., 2013; Fuentes and Arregui, 2009; Monteleone et al., 2012). PTP1B promotes acute integrin-dependent Src/FAK activation, modulation of Rho A/Rac 1 activities and myosin-dependent contractility (Burdisso et al., 2013; González Wusener et al., 2016). In the present work, we established bimolecular fluorescence complementation (BiFC) assays to directly examine the targeting of a substrate-trapping mutant of PTP1B to relevant tyrosines on paxillin and FAK, in the context of cell-matrix adhesion sites. Our findings suggest a direct regulation of PTP1B on paxillin, by targeting the tyrosine residues Y31 and Y118, which are heavily phosphorylated after adhesion. In addition, our results are consistent with a role for PTP1B in keeping the FAK Tyr-925 unphosphorylated and thus, as suggested by our electrostatic analysis, favoring the compact FAT conformation that is recognized by paxillin.

RESULTS

Bimolecular fluorescence complementation constructs

Paxillin and FAK are key components of cell-matrix adhesion sites (Byron and Frame, 2016; Deakin and Turner, 2008; Schaller, 2010). Paxillin is phosphorylated in response to cell-matrix adhesion in two tyrosines, Y31 and Y118 (Bellis et al., 1997; Burridge et al., 1992; Petit et al., 2000), by Src and FAK (Bellis et al., 1995; Schaller and Parsons, 1995; Schaller and Schaefer, 2001; Schaller et al., 1999). Although stimulation by several growth factors induces tyrosine dephosphorylation of paxillin by the protein tyrosine phosphatase SHP-2 (also known as PTPN11) (Brown and Turner, 2004; Ren et al., 2004; Zhang et al., 2004a), the identity of protein tyrosine phosphatases that regulate paxillin dephosphorylation in cell-matrix adhesion sites is presently unknown. PTP1B dephosphorylates paxillin in *in vitro* assays (Schaller and Parsons, 1995) and reduces total paxillin tyrosine phosphorylation when it is highly overexpressed in human embryo kidney epithelial 293-EBNA cells (Takino et al., 2003). However, our previous work in fibroblast cell lines with impaired PTP1B function, as well as in genetically deficient PTP1B knockout cells, showed a reduction of total paxillin tyrosine phosphorylation (Arregui et al., 1998; González Wusener et al., 2016). We have proposed a model in which PTP1B is required for activating Src, which alone or together with FAK, phosphorylates paxillin. The first prediction of the model was widely supported (Arias-Salgado et al., 2005; Bjorge et al., 2000; Cheng et al., 2001; Cortesio et al., 2008; Fan et al., 2015; González Wusener et al., 2016; Liang et al., 2005; Monteleone et al., 2012). However, there is not an assessment of PTP1B targeting directly to phosphorylated paxillin in cell-matrix adhesion sites. In addition, the putative PTP1B target tyrosine residues have not been identified.

FAK is tyrosine phosphorylated and activated in response to cell-matrix adhesion (Burridge et al., 1992; Guan and Shalloway, 1992; Lipfert et al., 1992). FAK clustering promotes its autophosphorylation at Y397 in the FERM-kinase linker and generates a binding site for the Src SH2 domain, which along with the Src SH3 domain binding to the first proline-rich motif, form a bidentate interaction that stabilizes the FAK-Src complex (Brami-Cherrier et al., 2014; Goñi et al., 2014; Katz et al., 2002; Schaller et al., 1994). Src phosphorylates FAK at several tyrosine residues, including Y576 and Y577 in the kinase activation loop, Y861 in the kinase-FAT linker and Y925 in the FAT domain (Brunton et al., 2005; Calalb et al., 1995; Lietha et al., 2007; Schlaepfer and Hunter, 1996b; Schlaepfer et al., 1994). Several protein tyrosine phosphatases have been implicated in FAK dephosphorylation (Cohen and Guan, 2005). When α-actinin 1 and PTP1B are overexpressed, the phosphorylation of FAK Y397 is negatively regulated (Zhang et al., 2006). These results are consistent with our recent BiFC data showing the presence of catalytic PTP1B D181A-α-actinin 1 complexes in cell-matrix adhesion sites (Burdisso et al., 2013).

To determine the role of PTP1B on paxillin and FAK localized in cell-matrix adhesions, we prepared a series of BiFC constructs of wild type and tyrosine to phenylalanine substitutions in paxillin and FAK (Fig. 1A). The N-terminus fragment of enhanced yellow fluorescent protein (YN_{1-154}) was fused to the N terminus of paxillin and FAK. The N-terminus tagging of paxillin did not affect the interactions of the C-terminus LIM domains with focal adhesion proteins and with the plasma membrane (Ripamonti et al., 2021). By performing paired co-transfections with YC-PTP1B D181A (named PTP1B DA from now on), these constructs allowed the direct visualization of intermediate catalytic complexes of PTP1B-paxillin and PTP1B-FAK at high spatial resolution using BiFC analysis in adhesions of intact cells. We have successfully used this technique before to visualize PTP1B complexes with Src (Monteleone et al., 2012) and α-actinin 1 (Burdisso et al., 2013). PTP1B DA refers to a PTP1B mutant in which the invariant Asp-181 involved in the tyrosyl phosphate cleavage has been replaced by alanine, converting the enzyme in a high-affinity substrate trap so that it is suitable for analyzing PTP-substrate interactions by microscopy (Flint et al., 1997; Haj et al., 2002). These interactions can be efficiently blocked by pervanadate, which binds to the catalytic cysteine of PTP1B and works as a competitive inhibitor (Huyer et al., 1997). We have previously reported that fusions of the C-terminus fragment of enhanced yellow fluorescent protein ($YC_{155-237}$) to PTP1B DA and the wild-type form both localize at the ER (Monteleone et al., 2012), as expected for the endogenous PTP1B (Frangioni et al., 1992) and full-length GFP-tagged constructs (Arregui et al., 1998; Haj et al., 2002; Hernández et al., 2006). We confirmed the correct expression and localization of all YN-paxillin and YN-FAK constructs to cell-matrix adhesions (Fig. 1B,C). The polyclonal anti-GFP labeled both YN and YC fragments with similar intensity, and in cells co-transfected with YC-PTP1B and YN-paxillin/FAK constructs facilitated the observation of the different signal distributions on the ER and in adhesions, respectively (Fig. S1). Cells expressing the BiFC constructs had total average levels of the correspondent protein (endogenous plus exogenous) that were double the levels of the endogenous protein in non-transfected cells (Fig. S2, only the most relevant YN-paxillin and YN-FAK constructs are shown).

PTP1B targets to phosphorylated paxillin in cell-matrix adhesion complexes

As PTP1B and paxillin localize to different compartments, the ER and cell-matrix adhesions, respectively, the BiFC signal was

Journal of Cell Science (2021) 134, jcs258769. doi:10.1242/jcs.258769

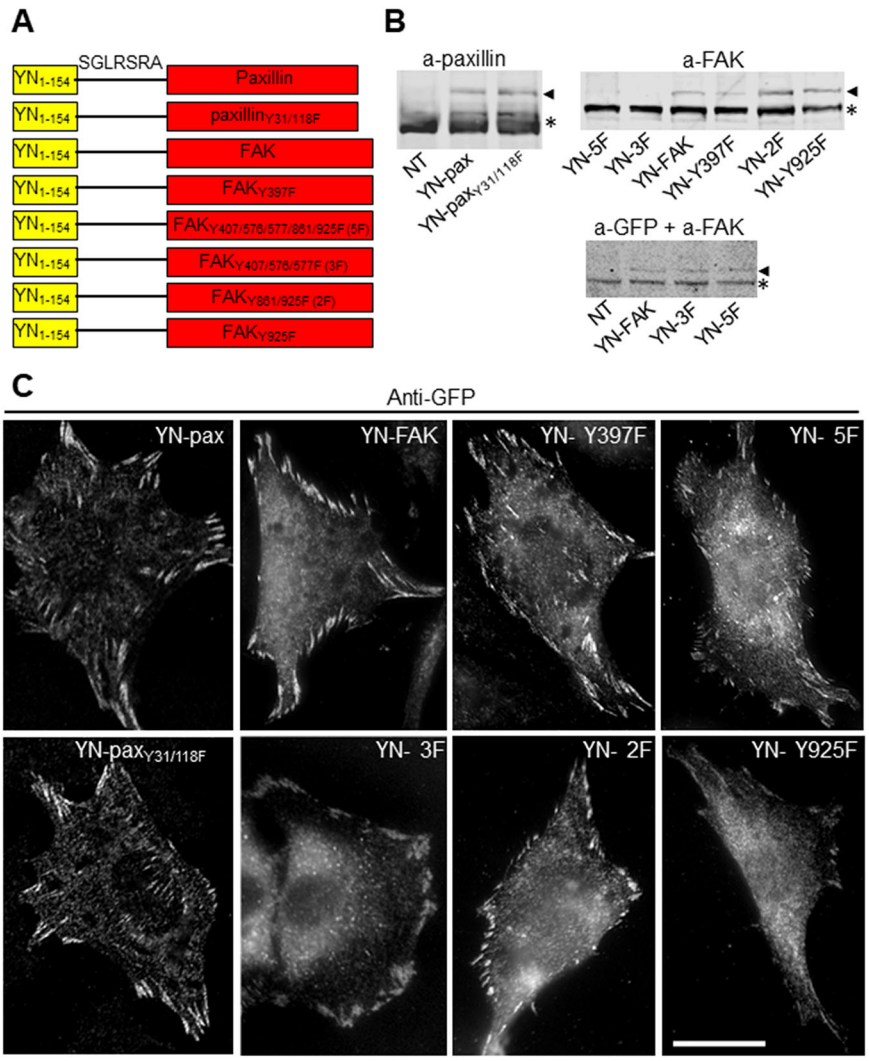

Fig. 1. Design and expression of BiFC constructs. (A) Diagram of the fusion proteins. YN fragment (residues 1-154) of enhanced YFP was fused to the amino terminus of paxillin, paxillin Y31/118F, FAK, FAK Y397F, FAK Y407/576/577/861/925F (named 'YN-5F'), FAK Y407/576/577F (named 'YN-3F'), FAK Y861/925F (named 'YN-2F') and FAK Y925F. The amino acids of the linker region are indicated in capital letters. (B) Constructs were transiently expressed in PTP1B wild-type cells and probed in western blots with anti-paxillin (upper left panel), anti-FAK (upper right panel) and anti-GFP simultaneously with anti-FAK (lower panel) antibodies. The YN fragment adds ∼18 kDa to the partner fused proteins (paxillin and FAK). Arrowheads indicate the migration of the fusion proteins, whereas asterisks indicate the migration of the endogenous proteins. Anti-FAK did not efficiently recognize FAK mutants YN-5F and YN-3F, probably due to an overlap with the protein region (amino acids 354-533) used as an immunogen. Thus, for these mutants, cell extracts were also probed with anti-GFP, which efficiently recognizes the YN fragment. (C) Subcellular distribution of the constructs used for BiFC was assessed by fluorescence microscopy. PTP1B wild-type cells expressing YN-paxillin, YN-paxillin Y31/118F, YN-FAK, YN-FAK 3F, YN-FAK Y397F, YN-FAK 2F, YN-FAK 5F and YN-FAK Y925F were immunolabeled with anti-GFP followed by Alexa Fluor 568-conjugated secondary antibody. Images on the red channel (not shown) indicate that all constructs localize in peripheral focal adhesions as expected. Scale bar: 25 µm.

analyzed in the context of markers for these compartments and after immunofluorescence detection of anti-PTP1B or anti-vinculin antibodies. Confocal optical sectioning of cells co-expressing YN-paxillin and YC-PTP1B DA (DA) revealed BiFC fluorescence only in sections of the cell in contact with the substratum (Fig. 2). The BiFC signal showed a pattern of peripheral diffraction-limited bright spots that frequently extended in less bright short segments (1-3 µm) that overlapped tightly (Manders' coefficient, >0.8) with anti-PTP1B fluorescence (Fig. 2A-F). The non-uniform distribution of BiFC within adhesions reflects the non-uniform distribution of phospho-paxillin (Fig. S3). The anti-PTP1B antibody revealed the typical distribution of the DA mutant in the ER network with peripheral bright spots, as shown previously (Haj et al., 2002; Hernández et al., 2006; Monteleone et al., 2012). The spots and segments of BiFC fluorescence overlapped with cell-matrix adhesions that were revealed by anti-vinculin antibody (Fig. 2G-L). A quantitative analysis showed that the BiFC signal overlapped with more than 90% of the total YC-DA spots. To confirm that BiFC signal depends on the trapping mutation introduced in the catalytic site of PTP1B (Flint et al., 1997), and not on a scaffolding effect, we performed a parallel analysis of BiFC using the YC-PTP1B wild-type construct, which has an intact catalytic site. In this condition, only a background BiFC signal was detected (Fig. 3A,B). Furthermore, preincubation of cells co-transfected with the DA/paxillin pair with sodium pervanadate significantly reduced the BiFC signal (Fig. 3E,F) compared to the same BiFC pair without the inhibitor (Fig. 3C,D). PTP1B may be recruited to paxillin indirectly by forming complexes with CrkII (Takino et al., 2003), which involve the polyproline motif of PTP1B and the SH3 domain of Crk (Liu et al., 1996). We examined the BiFC signal of the double mutant PTP1B DA-PA, in which the polyproline motif was disrupted and thus binding to the CrkII SH3 domain was reduced (Dadke and Chernoff, 2002). The BiFC signal of PTP1B DA-PA with paxillin did not differ significantly compared to PTP1B DA (Fig. S4A-D). Collectively, these data indicate that the active site of DA binds to tyrosyl phosphorylated paxillin within cell-matrix adhesions producing a positive BiFC signal. Additional experiments using the substrate trap DA failed to produce BiFC with vinculin (Fig. S4E,F), a prominent focal adhesion protein phosphorylated by Src (Niediek et al., 2012; Zhang et al., 2004b).

Cell adhesion-dependent phosphorylation of paxillin occurs mainly in tyrosine residues Y31 and Y118 (Bellis et al., 1997; Kuo et al., 2011; Schaller and Parsons, 1995; Schaller and Schaefer, 2001). As we previously have detected colocalization of GFP-DA puncta with paxillin-rich peripheral adhesions (Hernández et al., 2006), and BiFC shows a direct interaction with phosphorylated paxillin, we sought to identify whether these residues were targeted

Journal of Cell Science (2021) 134, jcs258769. doi:10.1242/jcs.258769

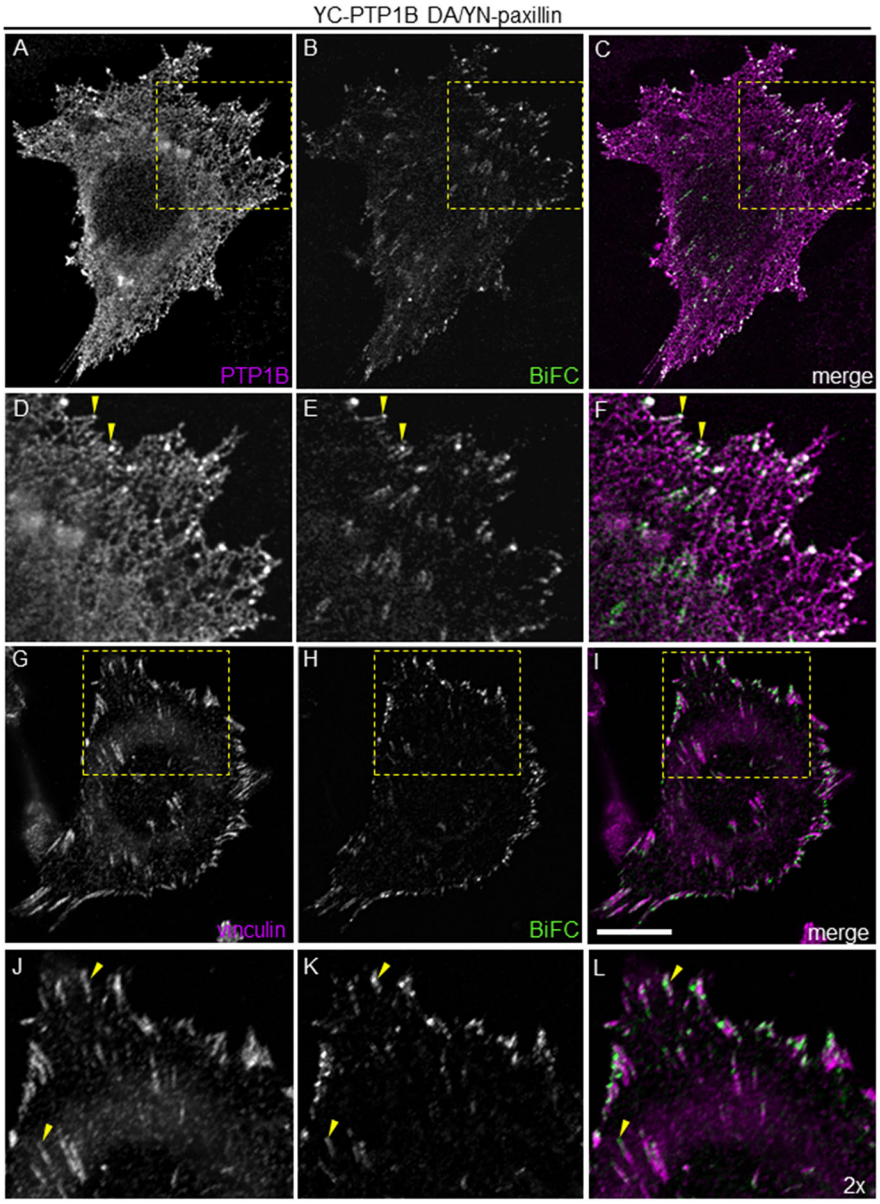

Fig. 2. BiFC distribution of the YC-PTP1B DA/YN-paxillin pair. PTP1B wild-type cells were co-transfected with YN-paxillin/YC-PTP1B DA and analyzed by confocal fluorescence microscopy. (A-C) Representative BiFC distribution of YC-PTP1B DA/YN-paxillin. Cells fixed and processed for immunofluorescence detection of PTP1B using Alexa Fluor 568-conjugated secondary antibodies are shown in magenta. (D-F) Magnifications of regions within boxes in A, B and C, respectively. Arrowheads indicate BiFC signal visualized as peripheral bright spots that overlap with YC-PTP1B DA distribution. (G-I) Representative BiFC distribution of YC-PTP1B DA/YN-paxillin in cells fixed and processed for immunofluorescence detection of vinculin, using Alexa Fluor 568-conjugated secondary antibodies in the red channel. (J-L) Magnifications of regions within boxes in G, H and I, respectively. Arrowheads indicate BiFC spots that overlap with cell-matrix adhesions labeled with anti-vinculin. The BiFC signal overlaps with the distal poles of the peripheral vinculin adhesions. For a better visualization of the ER and adhesions, images were sharpened using 'unsharp mask' from ImageJ. Scale bar: 20 µm.

by DA on paxillin. In cells co-expressing DA and paxillin mutants Y31F/Y118F, the BiFC signal was significantly reduced compared to that obtained with the DA/paxillin pair (Fig. 3G,H,M; Fig. S5). The anti-GFP signal confirmed the co-expression of both BiFC pair constructs (Fig. S1C).

FAK establishes complexes with, and phosphorylates, paxillin (Thomas et al., 1999). In addition, phosphorylated paxillin at Y31 and Y118 promotes FAK interaction (Choi et al., 2011; Zaidel-Bar et al., 2007). To determine whether the BiFC signal of DA/paxillin requires FAK localization to cell-matrix adhesions, we analyzed cells expressing the C-terminal domain of FAK, also called FAK-related non-kinase (FRNK). FRNK efficiently displaces endogenous FAK from focal adhesions and inhibits the tyrosine phosphorylation of paxillin (Richardson and Parsons, 1996). Consistently, we found that expression of myc-tagged FRNK reduced the DA/paxillin BiFC signal in adhesions to background levels (Fig. 3I,J), and this effect correlated with the reduced phosphorylation of paxillin (Fig. S6A-F). The levels of paxillin in adhesions were not affected by myc-FRNK expression (not shown). We further predicted a similar effect in FAK knockout cells (Ilić et al., 1995). FAK depletion by siRNA showed an inhibition of paxillin phosphorylation at Y31 and Y118 residues (Tilghman et al., 2005), an effect less evident in FAK knockout cells, likely due to compensatory effects by the FAK-related protein tyrosine kinase Pyk2 (Ilić et al., 1995; Lim et al., 2008). We co-expressed YN-paxillin and YC-DA in FAK knockout cells, and found a significant reduction of BiFC signal in cell-matrix adhesions (Fig. 3K,L), consistent with the reduction of pY118 in these cells (Fig. S6G-J). Taken together, these results indicate that PTP1B targets paxillin phosphorylated at Y31 and Y118 in cell-matrix adhesions, an event that is dependent on FAK activity.

PTP1B targets to phosphorylated FAK in cell-matrix adhesion complexes

FAK is phosphorylated on several tyrosine residues at cell-matrix adhesions (Ballestrem et al., 2006; Brunton et al., 2005; Kuo et al., 2011; Martínez et al., 2020; Nakamura et al., 2001; Ruest et al., 2000). Each phosphorylated FAK tyrosine residue plays a distinct functional role. Phosphorylation of Y397 converts this site into a

Journal of Cell Science (2021) 134, jcs258769. doi:10.1242/jcs.258769

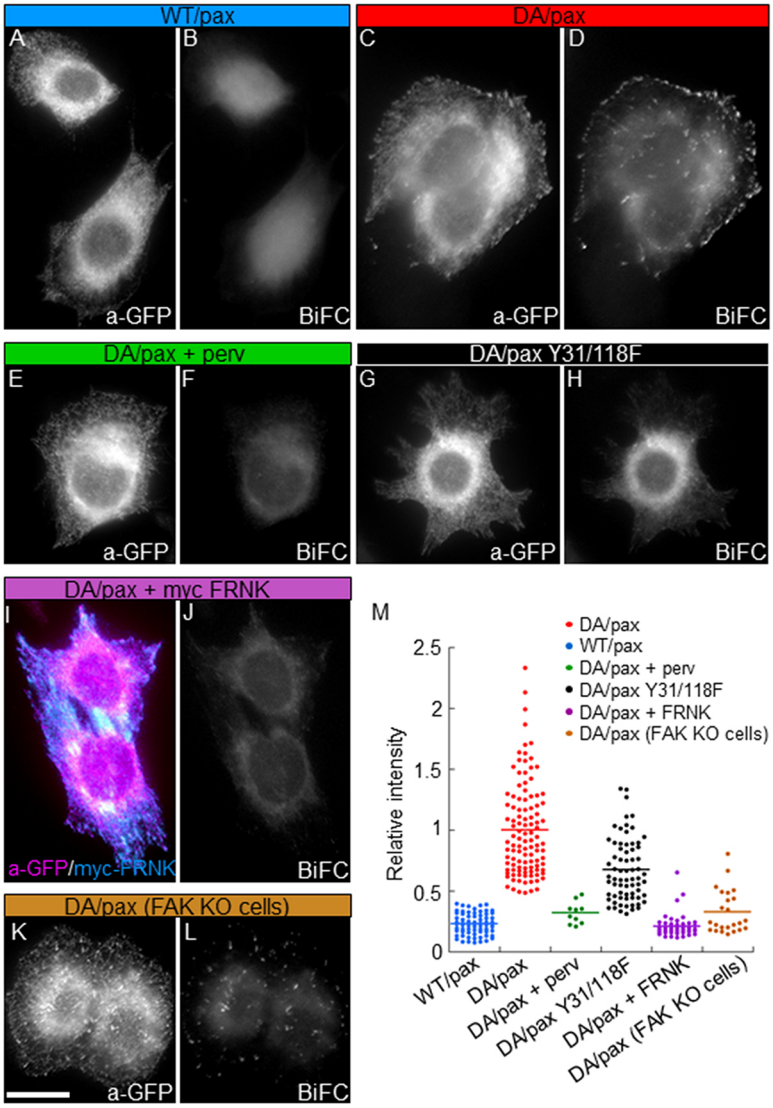

Fig. 3. BiFC of YC-PTP1B/YN-paxillin occurs under specific requirements. (A-L) PTP1B wild-type cells (A-J) and FAK knockout (KO) cells (K,L) were co-transfected and analyzed by fluorescence microscopy. Images of BiFC and anti-GFP signals in representative cells are shown for YC-PTP1B wild type (WT)/YN-paxillin (pax) (A,B), YC-PTP1B DA/YN-paxillin (C,D), YC-PTP1B DA/YN-paxillin in cells preincubated with pervanadate (perv) (E,F), YC-PTP1B DA/YN-paxillin Y31/118F (G,H) and YC-PTP1B DA/YN-paxillin in cells co-transfected with myc-FRNK (I,J). Images of BiFC and anti-GFP signals are shown for FAK knockout cells co-expressing YC-PTP1B DA/YN-paxillin (K,L). (M) The relative intensity of BiFC to GFP signal in peripheral cell-matrix adhesions for all the conditions was quantified. Each data point represents the average value of a cell. All ratios were normalized to the mean of DA/paxillin ratio. Wild type/paxillin, n=73; DA/paxillin, n=109; DA/paxillin plus pervanadate, n=10; DA/paxillin Y31/118F, n=72; DA/paxillin plus FRNK, n=46; FAK knockout DA/paxillin, n=24. The mean value is displayed as a line. DA/paxillin was compared to all other conditions (one-way ANOVA, P<0.0001). Scale bar: 30 µm.

high-affinity binding site for the Src SH2 domain, promoting Src recruitment into cell-matrix adhesions. Phosphorylation of Y576 and Y577 induces full catalytic activity of FAK. Phosphorylation of Y925 constitutes a docking site for the adaptor protein Grb2, which links to the activation of the mitogen-activated protein kinase (MAPK) signaling pathway. The role of Y407 and Y861 are less well defined, but likely perform a scaffolding function (Boivin et al., 2013; Eliceiri et al., 2002; le Boeuf et al., 2004; Lim et al., 2004). To determine the interaction of PTP1B with FAK in cell-matrix adhesions, we co-transfected cells with YC-DA and YN-FAK. Wide-field and confocal analysis revealed a strong BiFC signal, which overlapped with peripheral adhesions and was displayed as puncta at the distal pole of adhesions. BiFC puncta were frequently extended as a segment of lower brightness aligned with the major axis of adhesions. In flat peripheral extension of cells, the bright BiFC puncta overlapped with the tubular ER network (Fig. 4). Confocal sectioning also revealed that a fraction of BiFC puncta located at more central regions in the cell, corresponding to deeper planes away from the cell-substrate interphase. Quantitative analysis of BiFC using the YC-PTP1B wild-type construct showed a dim and diffuse background signal compared to that using the substrate trap YC-DA (Fig. 5A-D). In addition, the BiFC signal of YC-DA/YN-FAK was reduced to background levels in cells preincubated with sodium pervanadate (not shown). Thus, our data indicate that tyrosyl phosphorylated FAK is a bona fide substrate of PTP1B in cell-matrix adhesions.

To identify the tyrosine residues targeted by PTP1B, we performed phenylalanine substitutions of the major phosphorylated tyrosines in FAK. Previous work has shown that overexpression of α-actinin 1 and PTP1B in COS-7 cells and PTP1B-null fibroblasts is accompanied by a selective reduction in the phosphorylation of FAK Y397, whereas the phosphorylation of Y407, Y576, Y577, and Y861 was unaffected (Zhang et al., 2006). To determine whether the substrate trap YC-DA recognizes FAK Y397 in cell-matrix adhesions, we co-transfected cells with the YC-DA/YN-FAK Y397F pair. Observations and quantification of the BiFC signal showed that it was not different to that produced by the YC-DA/YN-FAK pair (Fig. 5E,F,O). Similar results were obtained when the triple YC-FAK Y407F/Y576F/Y577F mutant was used (Fig. 5G,H,O). In contrast, the quintuple YC-FAK Y407F/Y576F/Y577F/Y861F/Y925F mutant, the double YC-FAK Y861F/Y925F mutant and the single YC-FAK Y925F mutant all rendered background levels of BiFC (Fig. 5I-N,O). Collectively, these results indicate that PTP1B targets Y925 at the FAT domain of FAK in cell-matrix adhesions.

We further sought to determine the effect of PTP1B on the phosphorylation state of FAK Y925 in PTP1B knockout cells and

Journal of Cell Science (2021) 134, jcs258769. doi:10.1242/jcs.258769

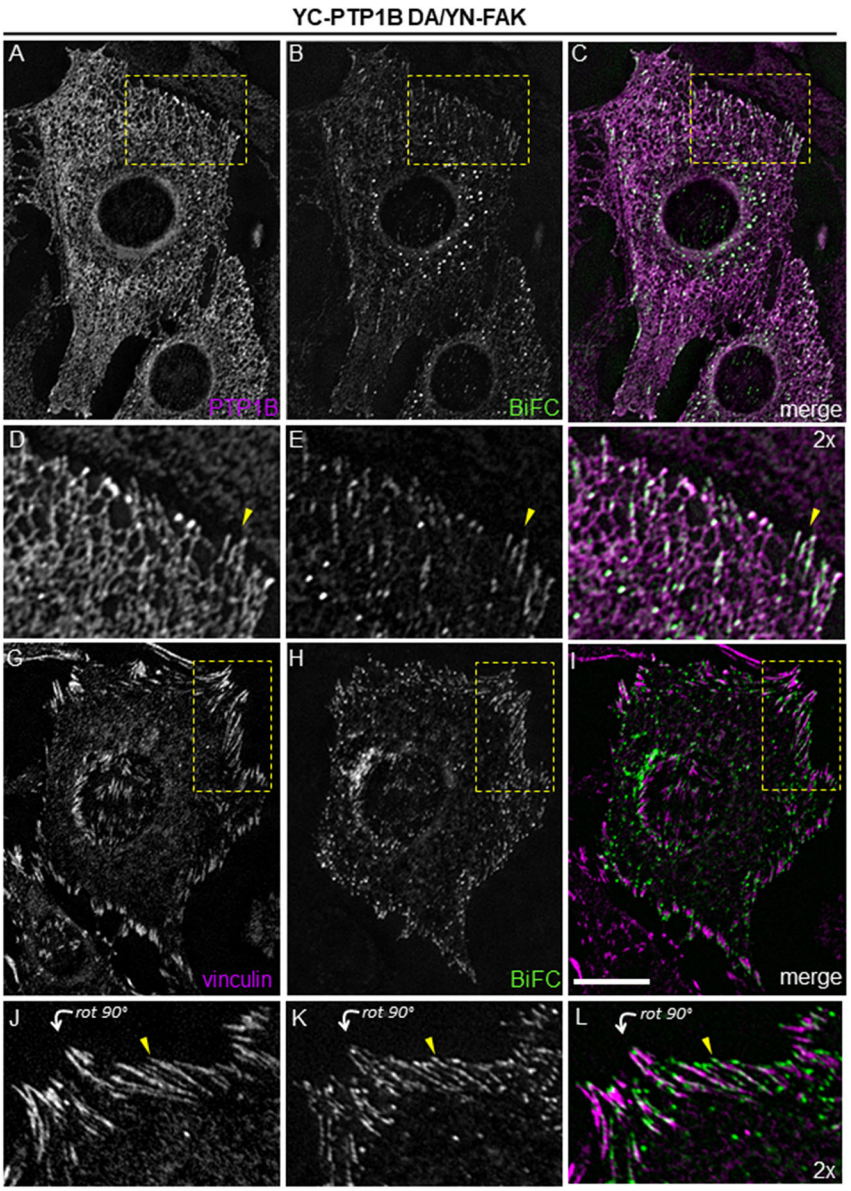

Fig. 4. BiFC distribution of the YC-PTP1B DA/YN-FAK pair. (A-L) PTP1B wild-type cells were co-transfected with YN-FAK/YC-PTP1B DA and analyzed by wide-field fluorescence microscopy. (A-C) Representative BiFC distribution of YC-PTP1B DA/YN-FAK. Cells fixed and processed for immunofluorescence detection of PTP1B, using Alexa Fluor 568-conjugated secondary antibodies are shown. (D-F) Magnifications of regions within boxes in A, B and C, respectively. Arrowheads indicate BiFC signal visualized as peripheral bright puncta that overlap with YC-PTP1B DA, following the tubular distribution of the ER. (G-I) Representative BiFC distribution of YC-PTP1B DA/YN-FAK in cells fixed and processed for immunofluorescence detection of vinculin, using Alexa Fluor 568-conjugated secondary antibodies. (K-L) Magnifications of regions within boxes in G, H and I, respectively. Arrowheads indicate BiFC puncta that overlap with the distal pole of cell-matrix adhesions labeled with anti-vinculin. Most BiFC signal extends as a lower brightness line along the major axis of the adhesions. For a better visualization of the ER and adhesions, images were sharpened using 'unsharp mask' from ImageJ. Scale bar: 20 µm.

knockout cells reconstituted with human wild-type PTP1B. Cells were processed for western blot analysis using a phospho-specific antibody against FAK pY925. The FAK-pY925/total FAK ratios did not differ significantly between wild-type and knockout cells (Fig. 6A). However, when a constitutively active mutant of Src (Src Y529F) was expressed, the pY925 levels in knockout cells were significantly higher than in wild-type cells. Thus, although a balance is maintained in wild-type cells, the increased phosphorylated state of FAK Y925 in knockout cells may reflect the lack of regulation by PTP1B. We further analyzed the link between pY925 and PTP1B in individual knockout cells reconstituted with GFP-PTP1B or GFP-PTP1B CS, an inactive mutant in which the catalytically essential cysteine 215 is replaced by serine (Guan and Dixon, 1991). Although cells expressing wild-type PTP1B display positive anti-FAK pY925 signal in adhesions, non-transfected cells or cells expressing the catalytically inactive (CS) mutant exhibited background levels (Fig. 6B-G). Alternatively, mouse embryonic fibroblasts transfected with the CS mutant, which has a dominant-negative effect on endogenous PTP1B (Arregui et al., 1998), showed reduced pY925 signal compared to non-transfected cells (Fig. 6H-J). These results indicate that PTP1B promotes the phosphorylation of FAK Y925, likely due to its well-established role as an activator of Src (Arias-Salgado et al., 2005; Bjorge et al., 2000; Cheng et al., 2001; Cortesio et al., 2008; Fan et al., 2015; González Wusener et al., 2016; Liang et al., 2005; Monteleone et al., 2012). As Src is the main kinase that phosphorylates FAK Y925 (Brunton et al., 2005; Schlaepfer and Hunter, 1997), it is expected that the reconstitution of SYF cells (triple knockout of Src, Yes and Fyn) with constitutively active Src-HA leads to robust pY925 signal in focal adhesions. Indeed, this effect was verified experimentally, and it is clearly absent in parental non-transfected cells (Fig. 6K-M). These results suggest that in conditions of Src overexpression, as frequently occurs in cancer (Irby and Yeatman, 2000; Oneyama and Okada, 2015; Wheeler et al., 2009), PTP1B may exert a protective role by keeping the low phosphorylation state of FAK Y925, which is compatible with cell adhesion to the extracellular matrix.

Next, we wanted to test whether the PTP1B effect on FAK Y925 reduces the signal flux leading to the activation of the Erk1/2 pathway. FAK mediates integrin and growth factor-dependent

Journal of Cell Science (2021) 134, jcs258769. doi:10.1242/jcs.258769

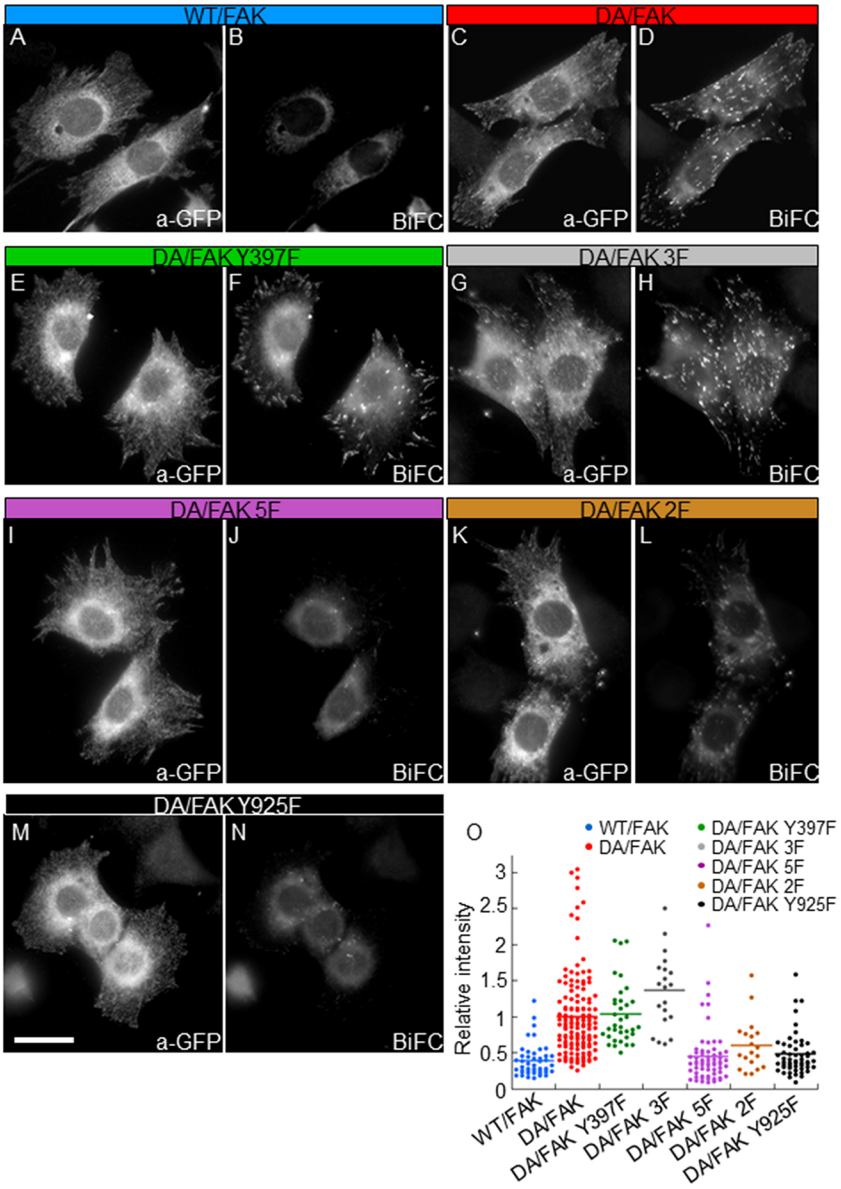

Fig. 5. BiFC analysis between YC-PTP1B and YN-FAK Tyr to Phe mutants. (A-N) PTP1B wild-type (WT) cells were co-transfected and analyzed by fluorescence microscopy. Images of BiFC and anti-GFP signals in representative cells are shown for YC-PTP1B WT/YN-FAK (A,B), YC-PTP1B DA/YN-FAK (C,D), YC-PTP1B DA/YN-FAK Y397F (E,F), YC-PTP1B DA/YN-FAK 3F (G,H), YC-PTP1B DA/YN-FAK 5F (I,J), YC-PTP1B DA/YN-FAK 2F (K,L) and YC-PTP1B DA/YN-FAK Y925F (M,N). (O) The relative intensity of BiFC to GFP signal in peripheral cell-matrix adhesions for all the conditions was quantified. Each data point represents the average value of a cell. All ratios were normalized to the mean of the DA/FAK ratio. Wild type/FAK, n=46; DA/FAK, n=141; DA/Y397F, n=35; DA/3F, n=20; DA/5F, n=62; DA/2F, n=19; DA/Y925F, n=54. The mean value is displayed as a line. DA/FAK was compared to all other conditions (one-way ANOVA, DA/FAK versus wild type/FAK, DA/5F, DA/Y925F, P<0.0001; DA/FAK versus DA/3F, DA/2F, P<0.01; DA/FAK versus DA/Y397F NS). Scale bar: 30 µm.

activation of the MAPK Erk2 through multiple pathways (Renshaw et al., 1999; Schlaepfer et al., 1994, 1999). As fibronectin adhesion stimulates Erk2 activation through a FAK phospho-Y925-Grb2-Ras pathway, we sought to analyze the levels of Erk activity in wild-type and knockout cells adhered to fibronectin, with or without overexpression of constitutively active Src. Western blots stained with phospho-specific antibodies against active Erk1/2 revealed no statistically significant difference in the p-Erk/Erk ratios between wild-type and knockout cells, either in the absence or presence of Src overexpression (Fig. S7). Our results suggest that PTP1B does not have a significant impact on typical Erk activation dependent on the FAK phospho-Y925-Grb2 interactions.

FAK and paxillin interactions in PTP1B wild-type and knockout cells

Our BiFC analysis shows that PTP1B targets phosphorylated Y925 on FAK; however, the BiFC signal has a wide distribution, suggesting a high cell-to-cell variability. In addition, western blots and immunofluorescence analysis revealed that FAK pY925 required PTP1B and Src activity (Fig. 6). Thus, we decided to analyze whether the differential FAK Y925 phosphorylation in PTP1B wild-type and knockout cells has consequences for the FAK-paxillin interactions at cell-matrix adhesion sites.

Structural analysis has revealed that FAK binding to paxillin requires the integrity of the four-helix bundle conformation of the FAT domain (Gao et al., 2004; Hayashi et al., 2002; Hoellerer et al., 2003; Liu et al., 2002). Further co-immunoprecipitation studies have established that in this conformation FAK Y925 is in the non-phosphorylated state (Deramaudt et al., 2011; Kadaré et al., 2015) and not accessible to tyrosine kinases (Arold, 2011). Conformational flexibility of the FAT domain allows the separation of helix 1 and the phosphorylation by Src family kinases (Arold et al., 2002; Martínez et al., 2020; Prutzman et al., 2004). Thus, we predicted that the presence of PTP1B in wild-type cells should favor FAK-paxillin interactions and that its absence in the knockout cells should have the opposite effect. We analyzed FAK-paxillin interactions by BiFC, after co-transfection with YC-FAK and YN-paxillin. In wild-type and knockout cells, the BiFC signal was variable among adhesions, with the presence of hot spots along the longitudinal axis of adhesions (Fig. 7G,H inset, arrows).

Journal of Cell Science (2021) 134, jcs258769. doi:10.1242/jcs.258769

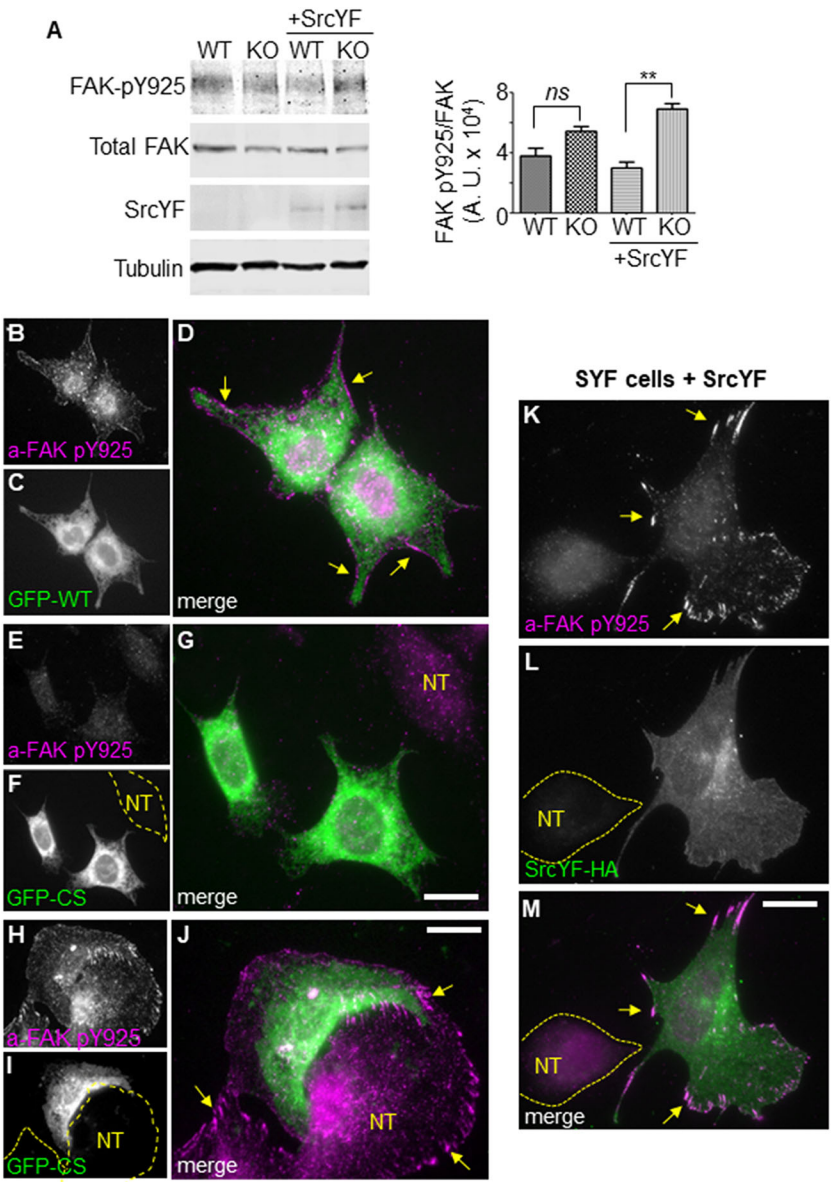

Fig. 6. PTP1B and Src activity regulate the phosphorylation state of FAK Y925. (A) Western blot analysis of PTP1B wild-type (WT) and knockout (KO) cells non-transfected and transfected with constitutive active SrcYF plated on fibronectin-coated dishes. Membranes were probed by antibodies against FAK pY925, FAK, GFP and tubulin. Three independent experiments were used for quantification using ImageJ software. pFAK values, normalized according to LI-COR published protocols, were used for the relative comparison of the different conditions. Data are mean±s.e.m. $^{**}P<0.01$; ns, not significant (unpaired two-tailed Student's *t*-test). (B-M) Immunofluorescence detection of FAK pY925 in individual cells. PTP1B knockout cells reconstituted with GFP-PTP1B wild type (B-D) or the catalytically inactive GFP-PTP1B CS (E-G). Arrows point to FAK pY925 in peripheral adhesions, only observed in cells expressing GFP-PTP1B wild type. Non-transfected (NT; dashed outlines) KO cells and cells expressing GFP-PTP1B CS did not show FAK pY925 label. (H-J) Mouse embryonic fibroblasts transfected with GFP-PTP1B CS. Arrows point to the FAK pY925 signal in adhesions of non-transfected cells. The signal is notably reduced in the transfected cell. (K-M) SYF cells transfected with the constitutively active SrcYF-HA. FAK pY925 in adhesions is robust only in the transfected cell (arrows). Scale bars: 20 µm. A. U., arbitrary units.

The average BiFC to GFP ratio in adhesions was quantified and revealed significantly higher values in wild-type cells compared to knockout cells (Fig. 7A-F,I). These results suggest that PTP1B promotes FAK-paxillin interactions in cell-matrix adhesion sites by dephosphorylation of FAK Y925, with a stabilizing effect on the compact (paxillin-binding competent) conformation of the FAT domain.

The phosphorylation state of Y925 affects the stability of the FAT 4-helix bundle

Nuclear magnetic resonance (NMR) and molecular dynamic simulations suggest that structural dynamics of the FAT domain leads to an alternative 'open' conformation in which helix 1 separates from the rest of the bundle and acquires the conformational freedom required for phosphorylation (Prutzman et al., 2004; Zhou et al., 2006), which is an observation that is consistent with crystallographic studies (Arold et al., 2002). The open conformation of the FAT domain prevents binding with paxillin (Kadaré et al., 2015), and the more extended conformation of helix 1 may satisfy the tyrosine kinase and Grb2 requirements for binding (Brown et al., 1999; Hubbard, 1997; Rahuel et al., 1996). As similar peptide conformations are bound by PTP1B (Jia et al., 1995; Salmeen et al., 2000), we predict that PTP1B binds to the phosphorylated Y925 in the open conformation of the FAT domain. Electrostatic analysis suggest that the four helices of the FAT domain tend to stabilize the bundle in a closed conformation due to the hydrophobic nature of their internal residues. To test the possibility that the phosphorylation of Y925 may affect this stability, we performed molecular dynamics simulations of FAT, both with Y925 in the unmodified and phosphorylated (pY925) state. We started from the open systems described in the Materials and Methods section, in which helix 1 is separated from the other three. After 500 ns simulations, helix 1, in both cases, tended to get closer to the rest of the bundle but did not reach a stable conformation, suggesting the possibility of a metastable open conformation (longer runs are needed to confirm this). Of note, there are several charged amino acids in the lower portion of helices 1, 2 and 4 (Fig. 8A). Helix 3 is ignored here as it is located further away from helix 1 and shielded by helices 2 and 4. These features prompted us to perform an electrostatic analysis of the last frame of the pY925 simulation using

Journal of Cell Science (2021) 134, jcs258769. doi:10.1242/jcs.258769

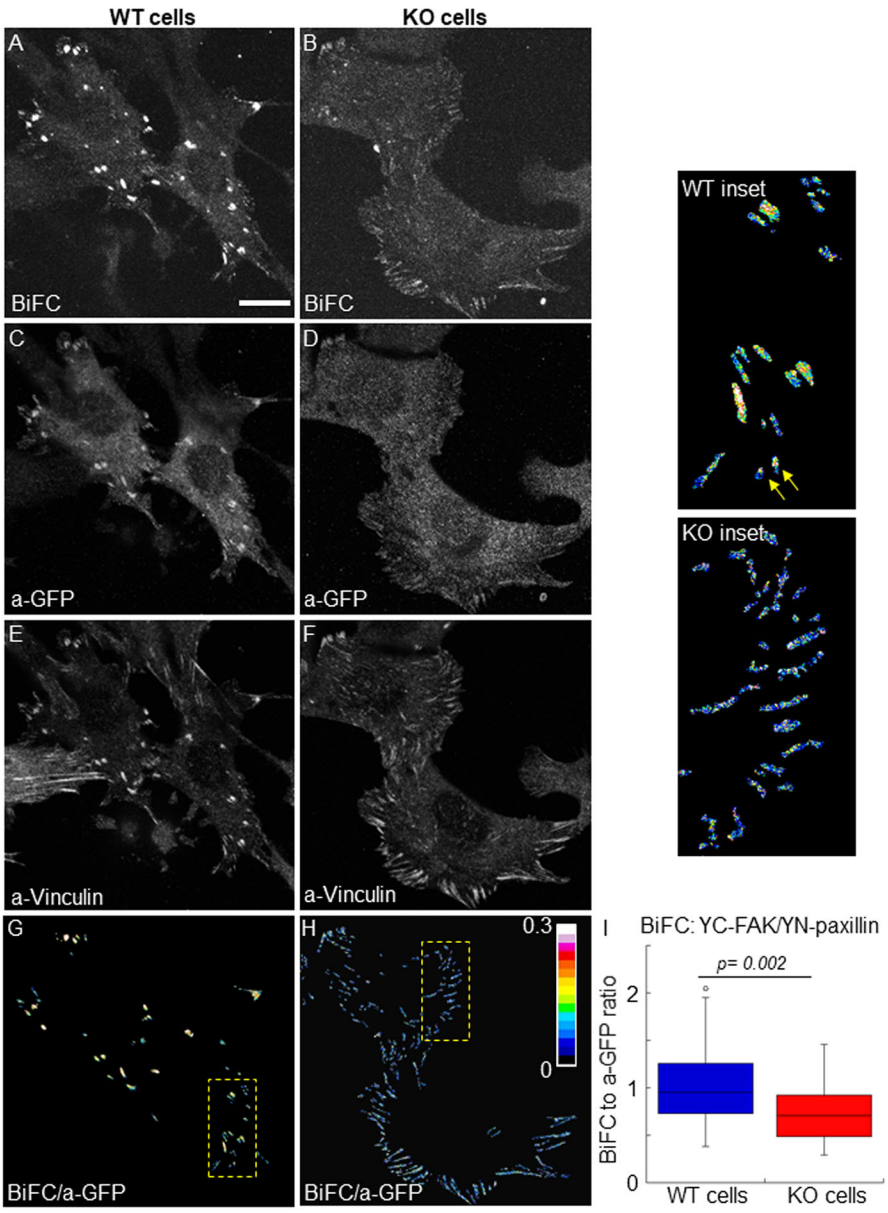

Fig. 7. BiFC analysis between YN-paxillin and YC-FAK in wild-type and knockout cells. (A-H) Fluorescence images of BiFC (A,B), anti-GFP (C,D) and anti-vinculin (E,F) signals in a representative PTP1B wild-type (WT) and PTP1B knockout (KO) cell are shown. Panels G and H show the BiFC to anti-GFP ratio of mean fluorescence intensities within segmented adhesions. Magnifications (3.5×) of the boxed areas in G and H are shown in the panels to the furthest right. Arrows point to BiFC hot spots in two small peripheral adhesions. Ratios are represented by a 16-color palette between a range of 0 to 0.3. (I) Box plots represent the mean values corresponding to BiFC/anti-GFP intensity ratios of all ROI per cell (n=45 for wild-type cells and 26 for KO cells). Boxes enclose 50% of the data with the median value displayed as a line. The top and bottom of the box mark the limits of the lower and upper quartiles. The lines extending from the top and bottom of each box mark the minimum and maximum values in the data set within 1.5 IQD (inter quartile distance) from the lower and upper quartiles, respectively. Any value outside of this range, called an outlier, is displayed as an individual point. Statistical significance between two non-normally distributed data groups was assessed by the Mann–Whitney test. Scale bar: 20 µm.

the Adaptive Poisson-Boltzmann Solver (APBS) software package for solving the corresponding Poisson-Boltzmann equation (Baker et al., 2001). The analysis was also performed on the same structure, but with an unphosphorylated tyrosine. In this way, it was possible to isolate the electrostatic effect of the phosphorylation, without interference from structural changes. The system with the unmodified residue showed an organized set of field lines connecting regions in helices 1 (mainly K923) and 2 (mainly E970), representing a strong attraction (Fig. 8B, left panel). On the other hand, in the system with the phosphorylated Y925 residue that organization was lost, and there was repulsion between the regions (Fig. 8B, right panel). This suggests a clear difference in the interactions developed by each case that could make the pY925 system more prone to keeping an open helix 1. To further confirm the relevance of these charged residues, we turned to an amino acid conservation calculation, as high conservation is indicative of functional relevance (Asciutto et al., 2021; Pullara et al., 2017). Thus, conservation of the involved amino acids was evaluated through the analysis of a multiple sequence alignment of FAT, consisting of 388 sequences. Table S1 shows that all amino acids have a significant degree of conservation and several have remarkably high scores (no significant co-evolution was found among them). The table also includes four amino acids of helix 4 that are highly conserved, although they do not show significant interactions in the APBS calculation, suggesting they are relevant and may develop strong interactions in other conformations. The above results – strong interactions and high conservation – underscore a functional relevance of the mentioned amino acids.

DISCUSSION

Here, we propose that two major components of cell-matrix adhesions, the scaffold protein paxillin and the protein tyrosine kinase FAK, are substrates targeted by ER-bound PTP1B *in situ*. We used BiFC, combined with the substrate-trapping mutant PTP1B DA, to directly visualize and analyze the catalytic complexes and characterize the target tyrosine residues within the substrates. Our results expand the repertoire of PTP1B substrates at integrin adhesions (Anderie et al., 2007; Burdisso et al., 2013; Monteleone

Journal of Cell Science (2021) 134, jcs258769. doi:10.1242/jcs.258769

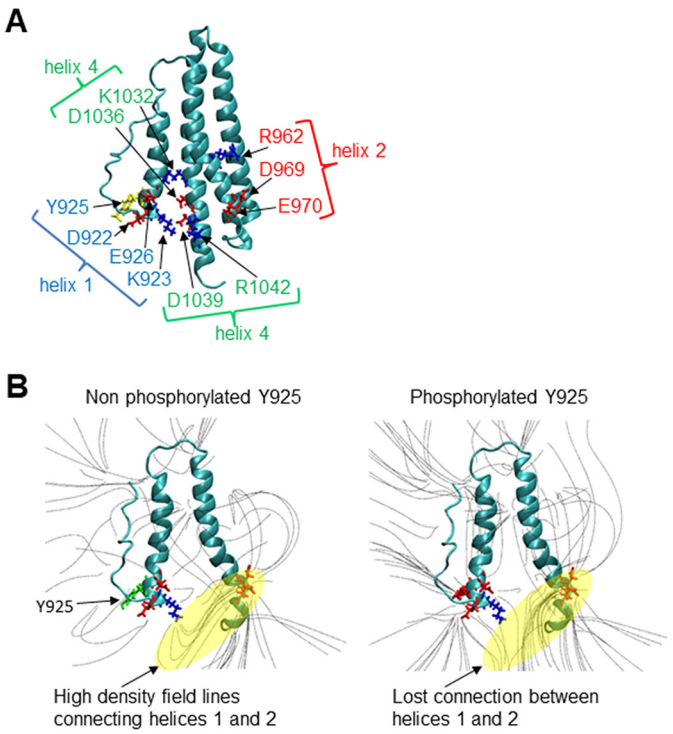

Fig. 8. Electrostatic analysis of FAT. (A) Schematic showing details of the charged residues located in helices 1, 2 and 4 in the interaction range of Y925 (yellow). (B) Electric field lines in the system (only showing the strongest interactions between helices 1 and 2) reveal a high density of lines connecting the bottom of helices 1 and 2 (left panel, Y925 in green), representing a strong electrostatic attraction (highlighted in yellow). This effect is reversed upon phosphorylation of Y925 (right panel, pY925 now is shown in red), and appears as a disconnection between the lines of each region. Charged residues generating those lines are shown.

et al., 2012) and reveal new regulatory mechanisms. The presence of PTP1B substrates in cell-matrix adhesions was previously suggested by the accumulation of the GFP-PTP1B DA but not GFP-PTP1B wild type in these sites (Hernández et al., 2006), which could be prevented by preincubation of cells with pervanadate, a general protein tyrosine phosphatase inhibitor that disrupts the trapping effect (Flint et al., 1997).

Many proteins of cell-matrix adhesions sites are phosphorylated by tyrosine (Ballestrem et al., 2006; Horton et al., 2016; Volberg et al., 2001; Zamir et al., 1999), and PTP1B is part of the phospho-adhesome network (Robertson et al., 2015). PTP1B is tail-anchored to ER membranes (Frangioni et al., 1992), and the peripheral distribution of these membranes allows PTP1B to regulate cell-matrix adhesion dynamics (Burdisso et al., 2013; Hernández et al., 2006; Ng et al., 2014; Zhang et al., 2010). However, the identification of substrates and potential mechanisms has advanced at a slow pace. Using BiFC, we have previously identified α-actinin-1 as one of such substrates regulated by PTP1B, likely promoting focal complex maturation and lamellar persistence (Burdisso et al., 2013). PTP1B has been implicated in paxillin and FAK dephosphorylation related to signaling that regulates cell migration (Liu et al., 1998; Takino et al., 2003; Zhang et al., 2006). However, to our knowledge, there has been no demonstration of PTP1B targeting to phosphorylated paxillin and FAK in cell-matrix adhesion sites, or identification of the putative tyrosine residues. The tyrosine kinase Src is a well-established PTP1B substrate that regulates adhesion (Arias-Salgado et al., 2005; Arregui et al., 1998; Bjorge et al., 2000; Cheng et al., 2001; Cortesio et al., 2008; Fan et al., 2015; González Wusener et al., 2016; Liang et al., 2005; Monteleone et al., 2012). However, PTP1B DA/Src complexes occur in punctate structures scattered throughout the cell-substrate surface, and are mostly excluded from cell-matrix adhesions (Monteleone et al., 2012). We have proposed a model in which ER-bound PTP1B activates membrane-associated Src in transient ER-plasma membrane contact sites, which is subsequently recruited to cell-matrix adhesions and, along with FAK, phosphorylates downstream substrates (Arregui et al., 2013). Paxillin residues Y31 and Y118 are robustly phosphorylated by Src and FAK early after cell adhesion (Bellis et al., 1995; Schaller and Parsons, 1995; Thomas et al., 1999; Tilghman et al., 2005; Fig. S8A). Our new results support this view, and further suggest that PTP1B counterbalances paxillin and FAK phosphorylation within adhesions complexes, particularly Y31 and Y118 in paxillin and Y925 in FAK (Fig. S8B). Highly phosphorylated paxillin is enriched in small focal complexes and at the more elongated focal adhesions (Ballestrem et al., 2006; Zaidel-Bar et al., 2007). The phosphorylation of paxillin is one factor that may modulate focal adhesion stability by promoting the integrin-cytoskeleton coupling (Ripamonti et al., 2021) and dynamics by FAK recruitment (Ishibe et al., 2004; Zaidel-Bar et al., 2007), although the mechanistic details are still unclear. Another factor is force. It has been suggested that paxillin phosphorylation at Y31 and Y118, and force, drive a maturation cycle during the lifetime of adhesion, which, after a time delay, induces paxillin dephosphorylation and the reduction of actomyosin contractility, causing adhesion weakening and disassembly (Pasapera et al., 2010; Schneider et al., 2009). Erk is recruited to newly formed focal complexes where it colocalizes with tyrosine phosphorylated paxillin (Ishibe et al., 2003). Erk phosphorylates paxillin creating a positive feedback loop by enhancing paxillin-FAK association and further phosphorylation of paxillin (Ishibe et al., 2004). Erk activity also promotes actomyosin contractility (Klemke et al., 1997; Pasapera et al., 2010), which in the assembly phase of the adhesion cycle may enhance FAK/Src-mediated paxillin phosphorylation (Pasapera et al., 2010). It is not clear how the transition between assembly and disassembly phases is regulated but it may occur by activation of negative feedback loops, such as the Erk-dependent phosphorylation of FAK at S910 of the FAT domain, an event that recruits the tyrosine phosphatase PTP-PEST to FAK and promotes dephosphorylation of FAK Y397 and inactivation (Zheng et al., 2009) (Fig. S8B). A substrate-trapping approach like that used in the present work reveals that p130Cas but not paxillin is the substrate of PTP-PEST (Shen et al., 2000). PTP-PEST directly binds to the LIM3/4-containing region of paxillin (Côté et al., 1999; Shen et al., 2000) and negatively modulates Rac1 activity and cell spreading (Jamieson et al., 2005; Lee et al., 2015; Sastry et al., 2002). The same paxillin region is required for FAT and interaction with kindlin (Brown and Turner, 2002; Theodosiou et al., 2016; Zhu et al., 2019), although it seems it is not required for targeting to β3 integrin-containing adhesions (Ripamonti et al., 2021), revealing integrin-dependent-specific functions of paxillin. The preference of PTP1B localization to adhesions containing β3 integrins (Arias-Salgado et al., 2005; González Wusener et al., 2016) may reflect different outcomes regulated by PTP1B and PTP-PEST; although the first promotes integrin- and Rac1-dependent spreading (Arregui et al., 1998; Burdisso et al., 2013; González Wusener et al., 2016), the second has the opposite effect (Angers-Loustau et al., 1999; Sastry et al., 2002).

We propose that PTP1B participates in an incoherent feedforward loop (IFFL) that tunes paxillin output depending on its phosphorylation. In an IFFL a protein simultaneously activates

Journal of Cell Science (2021) 134, jcs258769. doi:10.1242/jcs.258769

and inhibits a downstream protein via a direct and an indirect path (Alon, 2007). This configuration acts as a pulse generator and response accelerator. In our model (Fig. S8A), PTP1B in one path activates the tyrosine kinase Src, which then leads to paxillin Y31/Y118 phosphorylation at new adhesions, promoting their stability (Burdisso et al., 2013; González Wusener et al., 2016; Ripamonti et al., 2021). In a second kinetically slower path, PTP1B directly dephosphorylates paxillin (Fig. S8B). Dephosphorylation of paxillin by PTP1B could reduce the binding of paxillin to Erk (Ishibe et al., 2003). The dual effect of PTP1B on paxillin may modulate the cyclic assembly/disassembly behavior of adhesions and, at a larger scale, the cyclic membrane protrusions/retractions. In fact, PTP1B knockout cells significantly increase the protrusion/retraction switching frequencies of the leading edge compared to wild-type cells (Burdisso et al., 2013; Hernández et al., 2006). In addition, lifetimes of ER-PTP1B-targeted cell-matrix adhesions in protruding lamella (median of 20 min) are significantly longer than those that are not targeted (median of 4 min). Thus, the PTP1B-dependent IFFL may constitute a molecular network motif that regulates the 'timer' associated with adhesion lifetime and lamellar protrusions. Signaling from integrins and growth factor receptors may start the 'timer' converging in the activation of Src/FAK kinases and downstream Rho GTPases (Benlimame et al., 2005; DeMali et al., 2003; Huveneers and Danen, 2009; Lawson and Burridge, 2014; Schneider et al., 2009). We and others have demonstrated the specific role of PTP1B in integrin signaling, such as FAK and Src activation, paxillin and p130Cas phosphorylation, Rac1/RhoA modulation, and spreading (Arias-Salgado et al., 2005; Arregui et al., 1998; Burdisso et al., 2013; Cheng et al., 2001; González Wusener et al., 2016; Liang et al., 2005; Liu et al., 1998; Zhang et al., 2006). Notably, some of these effects caused by impairing PTP1B function were overridden or attenuated when cells are stimulated by serum, suggesting that serum components partly compensate for the lack of PTP1B (Arregui et al., 1998; Burdisso et al., 2013). Similarly, serum stimulation partially compensates the deficient cell spreading of FAK knockdown fibroblasts (Tilghman et al., 2005). Thus, the dual opposite effects of PTP1B on paxillin phosphorylation unraveled here in steady-state cells, in the presence of serum, underscore the complexities of local regulatory circuits and the need to integrate them under a wider systems biology perspective.

Our BiFC results also suggest that FAK is a substrate of PTP1B in cell-matrix adhesions and, although we did not explore further, likely also in endosomal compartments, consistent with the recent findings of FAK in this compartment (Alanko et al., 2015; Nader et al., 2016). Our detailed mutational analysis indicates that Y925, which is localized within the FAT domain of FAK, is the main target residue of PTP1B. This result is consistent with results of western blot and single-cell analysis using anti-FAK-pY925. The pY925 signal accumulates in cells in which Src is active, either by PTP1B expression or gain-of-function mutations on Src. X-ray crystallography and NMR spectroscopy showed that the FAT domain exists in two conformation states: a compact four-helix bundle, and an 'open' conformation in which helix 1 is separated from the rest of the bundle. In the open conformation, Y925 is exposed and more susceptible to phosphorylation and interaction with the SH2 domain of Grb2, promoting Erk activation (Brunton et al., 2005; Schlaepfer and Hunter, 1996a; Schlaepfer et al., 1994). In this conformation, the FAT domain cannot bind to paxillin (Kadaré et al., 2015). In contrast, the compact conformation interacts with LD motifs 2 and 4 of paxillin and excludes the phosphorylation of Y925 and Grb2 binding (Arold et al., 2002; Deramaudt et al., 2011; Hayashi et al., 2002; Hoellerer et al., 2003; Kadaré et al., 2015; Liu et al., 2002; Prutzman et al., 2004). Thus, the conformation dynamics and phosphorylation state of Y925 at the FAT domain establish a switch leading to different FAK outputs. Our BiFC analysis suggested that PTP1B promotes FAK binding to paxillin by ensuring the non-phosphorylated state of Y925, which facilitates the compact conformation of the FAT domain. This PTP1B function may be an additional layer of regulation promoting the structural stability of new focal complexes at cellular protrusions, in concordance with our previous findings (Burdisso et al., 2013). In addition, our molecular simulations clearly showed that phosphorylated Y925 may prevent the restoration of the closed 4-helix bundle due to the alteration of the electrostatic equilibrium between those regions. In this way, phosphorylation acts as a switch that can turn on or off the attraction between helices. This electrostatic picture is supported by the high conservation of the involved amino acids.

As proposed for paxillin, PTP1B may participate in an IFFL that tunes FAK Y925 output depending on its phosphorylation state. In our model, PTP1B in one path acts as an activator of the tyrosine kinase Src (Fig. S8A), which then leads to FAK phosphorylation at several tyrosine residues, including Y925 (Brunton et al., 2005), and in a second path PTP1B directly dephosphorylates this residue (Fig. S8B). The output of this IFFL may deliver pulse signals to the Erk pathway, as has been recently reported for Fyn and EGFR signaling (Albeck et al., 2013; Mukherjee et al., 2020; Sparta et al., 2015). In conclusion, our results indicate that paxillin and FAK are substrates regulated by PTP1B in cell-matrix adhesion sites and unravel new mechanisms for the modulation of actomyosin contractility by coupling positive and negative loops in a complex manner.

MATERIALS AND METHODS

DNA constructs

The amino fragment of EYFP, YN (residues 1-155), containing AgeI/BspEI as flanking restriction sites, was obtained by PCR from pEYFP-C1 plasmid and used to replace EGFP from pEGFP-C1 (Clontech BD Biosciences, Mountain View, CA, USA). The new plasmid pYN-C1 was used to generate YN fusions to the amino terminus of chicken FAK. YN-FAK and YN-FAK Y397F were prepared from GFP-FAK (Burdisso et al., 2013; Tilghman et al., 2005), amplifying the respective cDNAs with XhoI/BamHI flanking restriction sites to insert them into the pYN-C1 plasmid. Similarly, YN-FAK Y407/576/577/861/925F (named 'YN-5F') was obtained by PCR from pWZL-FAK 407-925F (Brunton et al., 2005). YN-FAK Y925F was generated by transferring the FAK NruI/BamHI fragment from YN-5F to YN-FAK. YN-FAK Y861/925F (named 'YN-2F') was obtained by transferring the FAK EcoRI/ApaI fragment from YN-FAK to YN-5F. YN-FAK Y407/576/577F (named 'YN-3F') was prepared by transferring the FAK EcoRI/ApaI fragment from YN-5F to YN-FAK. YN-paxillin Y31F/Y118F was generated from mRFP-human paxillin (Hernández et al., 2006) using the QuikChange site-mutagenesis kit (Stratagene). Paxillin and paxillin Y31F/Y118F cDNAs were amplified by PCR using XhoI/KpnI restriction sites to insert them into the pYN-C1 plasmid. YC-PTP1B wild-type/DA constructs for BiFC and constitutively active mouse SrcY529F-YN and Src Y529F-HA mutants (named as YF in the text) have been described previously (Monteleone et al., 2012). YC-PTP1B DA-PA was used as described previously (Monteleone et al., 2012). GFP-PTP1B wild type and the catalytically inactive PTP1B C215S (CS) were used as described previously (Arregui et al., 1998). pCMV-myc-FRNK was kindly provided by J. T. Parsons (University of Virginia, Charlottesville, VA, USA). All constructs were verified by sequencing.

Cell culture and DNA transfection

PTP1B wild-type and knockout cells were kindly provided by B. Neel (University Health Network, Toronto, Ontario, Canada; Haj et al., 2002).

SYF (triple knockout of Src, Yes and Fyn), FAK wild type and FAK knockout cell lines were purchased from the American Type Culture Collection (Manassas, VA, USA) and used as described previously (Burdisso et al., 2013). Mouse embryonic fibroblasts were kindly provided by P. Soriano (Fred Hutchinson Research Center, Seattle, WA, USA) (Klinghoffer et al., 1999). All cell lines, authenticated and free from contamination, were cultured in high glucose Dulbecco's modified Eagle medium containing L-glutamine, supplemented with 5% fetal bovine serum, penicillin and streptomycin (Invitrogen, Carlsbad, CA, USA) at 37°C and 5% CO_2. Transient transfections were performed in 24-well tissue culture plates using Lipofectamine 2000 (Invitrogen Corp, Carlsbad, CA, USA) and 0.5 µg of each construct per well. After 24 h, cells were resuspended and plated at a lower density on fibronectin (20 µg/ml)-coated coverslips (Paul Marienfeld, Lauda-Königshofen, Germany).

Antibodies and other labeling reagents

The monoclonal antibodies against PTP1B (Cat 610139, clone 15, used at 1:1000 dilution), paxillin (Cat 610051, clone 349, used at 1:2000 dilution) and FAK (Cat 610088, clone 77, used at 1:500 dilution) were obtained from BD Biosciences (Franklin Lakes, NJ, USA). Monoclonal anti-FAK (Cat MBS9602551) and polyclonal anti-FAK pY925 (Cat MBC821409) were purchased from MyBiosource (San Diego, CA, USA), and used at a dilution of 1:500. Polyclonal anti-calnexin (Cat C4731, used at 1:500 dilution), monoclonal anti-vinculin (Cat V9131, clone hVIN-1, used at 1:1000 dilution), anti-HA (Cat H9658, clone HA-7, used at 1:1000 dilution), anti-c-myc (Cat M5546, clone 9E10, used at 1:1000 dilution), monoclonal anti-alpha tubulin (Cat T9026, clone DM1A, used at 1:20,000) and anti-mouse IgG (Fc specific)-biotin antibody (Cat B7401, used at 1:400 dilution) were obtained from Sigma-Aldrich (St Louis, MO, USA). Monoclonal antibodies against Erk1/2 (Cat sc-514302, clone C-9) and phospho-Erk1/2 (Cat sc-136521, clone pT202/pY204.22A) (used at 1:500 dilution) were obtained from Santa Cruz Biotechnology (Dallas, TX, USA). Polyclonal antibodies against GFP (Cat A-6455, used at 1:2000 dilution), FAK-pY925 (Cat PA5-104965, used at 1:500 dilution), paxillin-pY118 (Cat 44-722G, used at 1:500) and Src (Cat 44656G, used at 1:1000 dilution) were purchased from Invitrogen (Carlsbad, CA, USA). Coumarin AMCA Streptavidin (Cat 016-150-084, used at 2 µg/ml) was obtained from Jackson ImmunoResearch (West Grove, PA, USA). Secondary antibodies used for western blotting were as follows: IRDye 680LT goat anti-mouse IgG (Cat 926-68020) or anti-rabbit IgG (Cat 926-68021), and IRDye 800CW goat anti-rabbit IgG (Cat 926-32211) (all used at 1:20,000 dilution and obtained from LI-COR Biosciences, Lincoln, NE, USA); and Alexa Fluor 488- and Alexa Fluor 568-conjugated secondary antibodies (Cat A-11008, A-11001, A-11011, A-11004, used at 1:700 dilution) (purchased from Invitrogen Carlsbad, CA, USA).

Immunofluorescence

Cells attached to fibronectin-coated coverslips (20 µg/ml) were sequentially fixed with 4% paraformaldehyde in PBS [137 mM NaCl, 2.7 mM KCl, 10 mM Na_2HPO_4 and 1.8 mM KH_2PO_4 (pH 7.4)] for 20 min, permeabilized with 0.5% Triton X-100/PBS for 5 min, and blocked in 3% bovine serum albumin (BSA)/PBS for 1 h. Primary and secondary antibodies were incubated at room temperature for 1 h. Samples were mounted in Vectashield (Vector Laboratories, Burlingame, CA, USA) and analyzed with a 60×1.4 NA objective in a Nikon TE2000-U microscope (Nikon Instruments, Melville, NY) coupled to an ORCA-AG cooled charged-coupled device camera (Hamamatsu Photonics, Hertfordshire, UK) or an Olympus IX81 Fluoview FV1000 confocal laser scanning microscope (Olympus, Tokyo, Japan). BiFC was analyzed with an excitation filter of 500/20 nm, an emission filter of 535/30 nm and an 86002v2bs dicroic mirror (Chroma Technology, Rockingham, VT, USA). In cells immunolabeled with Alexa Fluor 568-conjugated secondary antibody, BiFC and red signals were discriminated using the following Nikon filter sets: for BiFC, an excitation filter of 480/30 nm, an emission filter of 535/40 nm and a 505 longpass (LP) dicroic mirror; and for Alexa Fluor 568 nm, an excitation filter of 540/25 nm, an emission filter of 620/60 nm and a 565 (LP) dicroic mirror. In Fig. 3I, myc-FRNK was detected in the blue channel using an excitation filter of 360/40, an emission filter of 469/50 and a 400 (LP) dicroic mirror.

Processing and analysis of cell-matrix adhesions

ImageJ (version 1.50, National Institutes of Health) was used for all image processing and analysis procedures. For quantification of the BiFC signal in adhesions, images from wide-field and confocal microscopy (three summed slices of substrate sections), with an *xy* resolution of 0.10 µm/pixel were background subtracted using a rolling ball algorithm (Sternberg, 1983), with a rolling ball of 20 pixels radius. To measure mean intensity values from cell-matrix adhesions, binary masks were generated from copies of the original background-subtracted images and double immunolabeled for GFP and for adhesion markers (paxillin or vinculin). To facilitate the segmentation of adhesions, a mean-filtered image (radius 25 pixels) was subtracted from a median-filtered image (radius 1 pixel). An intensity threshold was applied to generate a binary image using the Otsu algorithm, and then particles smaller than 0.36 μm^2 were removed. The binary images of anti-GFP and the adhesion marker were color encoded (red/green) and merged to assess their matching (on yellow color). By way of a visual inspection of the merge image and of the original image overlaid with the outlines of regions of interest (ROI) obtained from the segmentation process, single-color scattered particles that were not part of adhesions were manually cleared in the merge image. In addition, adjacent adhesions that were classified as one ROI were split. Outlines of the final ROI in the merge binary image were overlaid on original images to visually confirm the faithful detection of signal from cell-matrix adhesions. Then, the mean intensity of the signal of the ROI was measured and computed. Intensity ratio images were obtained by dividing, pixel by pixel, the intensities in the YFP/GFP channel by those in the red channel. For statistical analysis, mean intensity ratio values were determined for each adhesion and copied into Excel spreadsheets. For image display, pixel ratio values were color encoded and displayed as a 16-color palette. To assess the expression levels of individual BiFC constructs (Fig. S2), extracellular ROI were subtracted from images containing transfected (T) and non-transfected (NT) cells, and then the average intensity of whole cells were determined using binary masks to identify transfected and non-transfected cells. For quantifications, at least 20 cells per condition were analyzed.

For the calculation of Manders' coefficients images were background subtracted and filtered (median filter of radius 2 pixels). The result images were analyzed with the plug-in JACOP (v2.0) using the default intensity threshold (Bolte and Cordelières, 2006).

Western blot analysis

Serum-starved wild-type and knockout cells attached on fibronectin-coated dishes (10 µg/ml) (1×10^6 cells per condition) for 20 and 60 min, or maintained in suspension for 30 min, were lysed on ice with TBS [20 mM Tris-HCl (pH 7.4), 137 mM NaCl] containing 1% Triton X-100, 2.5 mM $NaVO_3$, 10 mM NaF and protease inhibitor cocktail (Sigma-Aldrich). Cell lysates were centrifuged at 13,600 ***g*** for 15 min at 4°C, and ∼30 µg of the supernatants were fractionated by SDS-PAGE and transferred to a 0.45 µm pore size nitrocellulose membrane (Bio-Rad). After blocking with 3% BSA, membranes were probed with primary antibodies (2 µg/ml) followed by IRDye 680 or 800 secondary antibodies, and scanned with the Odyssey CLx infrared imaging system (LI-COR). Quantitative analysis of the signal intensity of the bands was performed using ImageJ according to the protocol 'Pan/Phospho Analysis for Western Blot Normalization' published by LI-COR. Briefly, the pan-protein and phosphoprotein signals were quantified using the Gel Analyzer from ImageJ. Then, the lane normalization factor (LNF) was calculated for each lane in the pan-protein signal, dividing each value with the highest signal for the total protein staining. Finally, the normalized phospho-target signal for each target band was calculated by dividing the target signal for each lane by the corresponding LNF. The normalized target protein values were used for relative comparison of the samples.

Molecular dynamics

The crystal structure (PDB 1K04) of the open conformation of chick FAK FAT domains (Arold et al., 2002) was used to build the initial model. The

simulations were performed using the AMBER18 (Case et al., 2018) software package, with all of them, except for the minimizations, using the GPU version of the PMEMD program, and the Amber 14 force field (Maier et al., 2015) was employed. The protocol followed for minimization and equilibration was: (1) 5000 cycles of minimization using the steepest descent method, followed by another 5000 steps using conjugate gradient; (2) 100 ps of heating to 300 K, using a Berendsen thermostat with a collision frequency of 2 ps^{-1}; (3) three 10 ns runs with constant T (300 K) and P (1 atm) run, using a weak-coupling Berendsen barostat with a relaxation time of 2 ps; and (4) a final equilibration in the NVT ensemble (constant volume and temperature) of 10 ns. The SHAKE algorithm was adopted in all simulations, allowing the use of a 2 fs time step, and long-range electrostatics were taken into account using periodic boundary conditions, via the Particle Mesh Ewald algorithm (Darden et al., 1993), with a cutoff of the sums in direct space of 10 Å. This protocol was repeated for another system, built in the same way, but in which residue Y925 was phosphorylated (pY925) (using the PTR phosphorylated amino acid, present in the ff14SB force field). The succeeding production runs were performed in the NVT ensemble, with durations of 500 ns each.

Conservation analysis

Starting with the sequence of the FAT domain, as appearing in the 1K05 PDB structure, a multiple sequence alignment composed of 388 sequences was built using the ConSurf server (Ashkenazy et al., 2016). Using in-house software, the conservation (Shannon's entropy) of amino acids occurring in that multiple sequence alignment was calculated, as was the sequence co-evolution, via the average-product-corrected mutual information (MIp) method (Dunn et al., 2008).

Statistical analysis

Statistical significance analysis was performed using GraphPad Prism 5. Analysis between multiple groups in Fig. 3 and Fig. 5 was determined using one-way ANOVA followed by the Dunnett's multiple comparison post-hoc test using the DA/pax column as the control. In all cases, $P<0.05$ was considered statistically significant.

Acknowledgements

We thank Dr Juan Burdisso for preparing the paxillin Y31F/Y118F mutant.

Competing interests

The authors declare no competing or financial interests.

Author contributions

Conceptualization: I.J.G., C.O.A.; Methodology: A.E.G.W., A.G., M.E.P.C., M.R.M., I.J.G., C.O.A.; Software: I.J.G., C.O.A.; Validation: C.O.A.; Formal analysis: A.E.G.W., A.G., M.R.M., I.J.G., C.O.A.; Investigation: A.E.G.W., A.G., M.E.P.C., M.R.M., I.J.G., C.O.A.; Resources: I.J.G., C.O.A.; Data curation: I.J.G., C.O.A.; Writing - original draft: I.J.G., C.O.A.; Writing - review & editing: A.E.G.W., C.O.A.; Visualization: A.E.G.W., C.O.A.; Supervision: I.J.G., C.O.A.; Project administration: C.O.A.; Funding acquisition: C.O.A.

Funding

This study was supported by the Consejo Nacional de Investigaciones Científicas y Técnicas to A.E.G.W., A.G., M.E.P.C., I.J.G., C.O.A. and the Agencia Nacional de Promoción Científica y Tecnológica (PICT 0826 to C.O.A.).

Peer review history

The peer review history is available online at https://journals.biologists.com/jcs/article-lookup/doi/10.1242/jcs.258769.

References

Alanko, J., Mai, A., Jacquemet, G., Schauer, K., Kaukonen, R., Saari, M., Goud, B. and Ivaska, J. (2015). Integrin endosomal signalling suppresses anoikis. *Nat. Cell Biol.* **17**, 1412-1421. doi:10.1038/ncb3250

Albeck, J. G., Mills, G. B. and Brugge, J. S. (2013). Frequency-modulated pulses of ERK activity transmit quantitative proliferation signals. *Mol. Cell* **49**, 249-261. doi:10.1016/j.molcel.2012.11.002

Alon, U. (2007). Network motifs: theory and experimental approaches. *Nat. Rev. Genet.* **8**, 450-461. doi:10.1038/nrg2102

Anderie, I., Schulz, I. and Schmid, A. (2007). Direct interaction between ER membrane-bound PTP1B and its plasma membrane-anchored targets. *Cell. Signal.* **19**, 582-592. doi:10.1016/j.cellsig.2006.08.007

Angers-Loustau, A., Côté, J.-F., Charest, A., Dowbenko, D., Spencer, S., Lasky, L. A. and Tremblay, M. L. (1999). Protein tyrosine phosphatase-PEST regulates focal adhesion disassembly, migration, and cytokinesis in fibroblasts. *J. Cell Biol.* **144**, 1019-1031. doi:10.1083/jcb.144.5.1019

Arias-Salgado, E. G., Haj, F., Dubois, C., Moran, B., Kasirer-Friede, A., Furie, B. C., Furie, B., Neel, B. G. and Shattil, S. J. (2005). PTP-1B is an essential positive regulator of platelet integrin signaling. *J. Cell Biol.* **170**, 837-845. doi:10.1083/jcb.200503125

Arold, S. T. (2011). How focal adhesion kinase achieves regulation by linking ligand binding, localization and action. *Curr. Opin. Struct. Biol.* **21**, 808-813. doi:10.1016/j.sbi.2011.09.008

Arold, S. T., Hoellerer, M. K. and Noble, M. E. M. (2002). The structural basis of localization and signaling by the focal adhesion targeting domain. *Structure* **10**, 319-327. doi:10.1016/S0969-2126(02)00717-7

Arregui, C. O., Balsamo, J. and Lilien, J. (1998). Impaired integrin-mediated adhesion and signaling in fibroblasts expressing a dominant-negative mutant PTP1B. *J. Cell Biol.* **143**, 861-873. doi:10.1083/jcb.143.3.861

Arregui, C. O., González, Á., Burdisso, J. E. and Wusener, A. E. G. (2013). Protein tyrosine phosphatase PTP1B in cell adhesion and migration. *Cell Adhes. Migr.* **7**, 418-423. doi:10.4161/cam.26375

Asciutto, E. K., Pantano, S. and General, I. J. (2021). Physical interactions driving the activation/inhibition of calcium/calmodulin dependent protein kinase II. *J. Mol. Graph. Model.* **105**, 107875. doi:10.1016/j.jmgm.2021.107875

Ashkenazy, H., Abadi, S., Martz, E., Chay, O., Mayrose, I., Pupko, T. and Ben-Tal, N. (2016). ConSurf 2016: an improved methodology to estimate and visualize evolutionary conservation in macromolecules. *Nucleic Acids Res.* **44**, W344-W350. doi:10.1093/nar/gkw408

Baker, N. A., Sept, D., Joseph, S., Holst, M. J. and McCammon, J. A. (2001). Electrostatics of nanosystems: application to microtubules and the ribosome. *Proc. Natl. Acad. Sci. USA* **98**, 10037-10041. doi:10.1073/pnas.181342398

Ballestrem, C., Erez, N., Kirchner, J., Kam, Z., Bershadsky, A. and Geiger, B. (2006). Molecular mapping of tyrosine-phosphorylated proteins in focal adhesions using fluorescence resonance energy transfer. *J. Cell Sci.* **119**, 866-875. doi:10.1242/jcs.02794

Bellis, S. L., Miller, J. T. and Turner, C. E. (1995). Characterization of tyrosine phosphorylation of paxillin in vitro by focal adhesion kinase. *J. Biol. Chem.* **270**, 17437-17441. doi:10.1074/jbc.270.29.17437

Bellis, S. L., Perrotta, J. A., Curtis, M. S. and Turner, C. E. (1997). Adhesion of fibroblasts to fibronectin stimulates both serine and tyrosine phosphorylation of paxillin. *Biochem. J.* **325**, 375-381. doi:10.1042/bj3250375

Benlimame, N., He, Q., Jie, S., Xiao, D., Xu, Y. J., Loignon, M., Schlaepfer, D. D. and Alaoui-Jamali, M. A. (2005). FAK signaling is critical for ErbB-2/ErbB-3 receptor cooperation for oncogenic transformation and invasion. *J. Cell Biol.* **171**, 505-516. doi:10.1083/jcb.200504124

Bjorge, J. D., Pang, A. and Fujita, D. J. (2000). Identification of protein-tyrosine phosphatase 1B as the major tyrosine phosphatase activity capable of dephosphorylating and activating c-Src in several human breast cancer cell lines. *J. Biol. Chem.* **275**, 41439-41446. doi:10.1074/jbc.M004852200

Boivin, B., Chaudhary, F., Dickinson, B. C., Haque, A., Pero, S. C., Chang, C. J. and Tonks, N. K. (2013). Receptor protein-tyrosine phosphatase α regulates focal adhesion kinase phosphorylation and ErbB2 oncoproteinmediated mammary epithelial cell motility. *J. Biol. Chem.* **288**, 36926-36935. doi:10.1074/jbc.M113.527564

Bolte, S. and Cordelières, F. P. (2006). A guided tour into subcellular colocalization analysis in light microscopy. *J. Microsc.* **224**, 213-232. doi:10.1111/j.1365-2818.2006.01706.x

Brami-Cherrier, K., Gervasi, N., Arsenieva, D., Walkiewicz, K., Boutterin, M.-C., Ortega, A., Leonard, P. G., Seantier, B., Gasmi, L., Bouceba, T. et al. (2014). FAK dimerization controls its kinase-dependent functions at focal adhesions. *EMBO J.* **33**, 356-370. doi:10.1002/embj.201386399

Braniš, J., Pataki, C., Spörrer, M., Gerum, R. C., Mainka, A., Cermak, V., Goldmann, W. H., Fabry, B., Brabek, J. and Rosel, D. (2017). The role of focal adhesion anchoring domains of CAS in mechanotransduction. *Sci. Rep.* **7**, 46233. doi:10.1038/srep46233

Brown, M. C. and Turner, C. E. (2002). Roles for the tubulin- and PTP-PEST-binding paxillin LIM domains in cell adhesion and motility. *Int. J. Biochem. Cell Biol.* **34**, 855-863. doi:10.1016/S1357-2725(01)00154-6

Brown, M. C. and Turner, C. E. (2004). Paxillin: adapting to change. *Physiol. Rev.* **84**, 1315-1339. doi:10.1152/physrev.00002.2004

Brown, N. R., Noble, M. E. M., Endicott, J. A. and Johnson, L. N. (1999). The structural basis for specificity of substrate and recruitment peptides for cyclin-dependent kinases. *Nat. Cell Biol.* **1**, 438-443. doi:10.1038/15674

Brunton, V. G., Avizienyte, E., Fincham, V. J., Serrels, B., Metcalf, C. A., Sawyer, T. K. and Frame, M. C. (2005). Identification of Src-specific phosphorylation site on focal adhesion kinase: dissection of the role of Src SH2 and catalytic functions and their consequences for tumor cell behavior. *Cancer Res.* **65**, 1117-1123. doi:10.1158/0008-5472.CAN-04-1949

Burdisso, J. E., González, Á. and Arregui, C. O. (2013). PTP1B promotes focal complex maturation, lamellar persistence and directional migration. *J. Cell Sci.* **126**, 1820-1831. doi:10.1242/jcs.118828

Burridge, K., Turner, C. E. and Romer, L. H. (1992). Tyrosine phosphorylation of paxillin and pp125FAK accompanies cell adhesion to extracellular matrix: a role in cytoskeletal assembly. *J. Cell Biol.* **119**, 893-903. doi:10.1083/jcb.119.4.893

Burridge, K., Sastry, S. K. and Sallee, J. L. (2006). Regulation of cell adhesion by protein-tyrosine phosphatases: I. Cell-matrix adhesion. *J. Biol. Chem.* **281**, 15593-15596. doi:10.1074/jbc.R500030200

Byron, A. and Frame, M. C. (2016). Adhesion protein networks reveal functions proximal and distal to cell-matrix contacts. *Curr. Opin. Cell Biol.* **39**, 93-100. doi:10.1016/j.ceb.2016.02.013

Byron, A., Askari, J. A., Humphries, J. D., Jacquemet, G., Koper, E. J., Warwood, S., Choi, C. K., Stroud, M. J., Chen, C. S., Knight, D. et al. (2015). A proteomic approach reveals integrin activation state-dependent control of microtubule cortical targeting. *Nat. Commun.* **6**, 6135. doi:10.1038/ncomms7135

Calalb, M. B., Polte, T. R. and Hanks, S. K. (1995). Tyrosine phosphorylation of focal adhesion kinase at sites in the catalytic domain regulates kinase activity: a role for Src family kinases. *Mol. Cell. Biol.* **15**, 954-963. doi:10.1128/MCB.15.2.954

Case, L. B., Baird, M. A., Shtengel, G., Campbell, S. L., Hess, H. F., Davidson, M. W. and Waterman, C. M. (2015). Molecular mechanism of vinculin activation and nanoscale spatial organization in focal adhesions. *Nat. Cell Biol.* **17**, 880-892. doi:10.1038/ncb3180

Case, D. A., Walker, R. C., Cheatham, T. E., Simmerling, C., Roitberg, A., Merz, K. M., Luo, R. and Darden, T. (2018). *Amber 2018*. University of California, San Francisco.

Cheng, A., Bal, G. S., Kennedy, B. P. and Tremblay, M. L. (2001). Attenuation of adhesion-dependent signaling and cell spreading in transformed fibroblasts lacking protein tyrosine phosphatase-1B. *J. Biol. Chem.* **276**, 25848-25855. doi:10.1074/jbc.M009734200

Choi, C. K., Zareno, J., Digman, M. A., Gratton, E. and Horwitz, A. R. (2011). Cross-correlated fluctuation analysis reveals phosphorylation-regulated paxillin-fak complexes in nascent adhesions. *Biophys. J.* **100**, 583-592. doi:10.1016/j.bpj.2010.12.3719

Cohen, L. and Guan, J.-L. (2005). Mechanisms of focal adhesion kinase regulation. *Curr. Cancer Drug Targets* **5**, 629-643. doi:10.2174/156800905774932798

Cortesio, C. L., Chan, K. T., Perrin, B. J., Burton, N. O., Zhang, S., Zhang, Z.-Y. and Huttenlocher, A. (2008). Calpain 2 and PTP1B function in a novel pathway with Src to regulate invadopodia dynamics and breast cancer cell invasion. *J. Cell Biol.* **180**, 957-971. doi:10.1083/jcb.200708048

Côté, J.-F., Turner, C. E. and Tremblay, M. L. (1999). Intact LIM 3 and LIM 4 domains of paxillin are required for the association to a novel polyproline region (Pro 2) of protein-tyrosine phosphatase-PEST. *J. Biol. Chem.* **274**, 20550-20560. doi:10.1074/jbc.274.29.20550

Dadke, S. and Chernoff, J. (2002). Interaction of protein tyrosine phosphatase (PTP) 1B with its substrates is influenced by two distinct binding domains. *Biochem. J.* **364**, 377-383. doi:10.1042/bj20011372

Darden, T., York, D. and Pedersen, L. (1993). Particle mesh Ewald: An N·log(N) method for Ewald sums in large systems. *J. Chem. Phys.* **98**, 10089-10092. doi:10.1063/1.464397

Deakin, N. O. and Turner, C. E. (2008). Paxillin comes of age. *J. Cell Sci.* **121**, 2435-2444. doi:10.1242/jcs.018044

DeMali, K. A., Wennerberg, K. and Burridge, K. (2003). Integrin signaling to the actin cytoskeleton. *Curr. Opin. Cell Biol.* **15**, 572-582. doi:10.1016/S0955-0674(03)00109-1

Deramaudt, T. B., Dujardin, D., Hamadi, A., Noulet, F., Kolli, K., de Mey, J., Takeda, K. and Rondé, P. (2011). FAK phosphorylation at Tyr-925 regulates cross-talk between focal adhesion turnover and cell protrusion. *Mol. Biol. Cell* **22**, 964-975. doi:10.1091/mbc.e10-08-0725

Dunn, S. D., Wahl, L. M. and Gloor, G. B. (2008). Mutual information without the influence of phylogeny or entropy dramatically improves residue contact prediction. *Bioinformatics* **24**, 333-340. doi:10.1093/bioinformatics/btm604

Eliceiri, B. P., Puente, X. S., Hood, J. D., Stupack, D. G., Schlaepfer, D. D., Huang, X. Z., Sheppard, D. and Cheresh, D. A. (2002). Src-mediated coupling of focal adhesion kinase to integrin αvβ5 in vascular endothelial growth factor signaling. *J. Cell Biol.* **157**, 149-160. doi:10.1083/jcb.200109079

Fan, G., Aleem, S., Yang, M., Miller, W. T. and Tonks, N. K. (2015). Protein-tyrosine phosphatase and kinase specificity in regulation of SRC and breast tumor kinase. *J. Biol. Chem.* **290**, 15934-15947. doi:10.1074/jbc.M115.651703

Flint, A. J., Tiganis, T., Barford, D. and Tonks, N. K. (1997). Development of "substrate-trapping" mutants to identify physiological substrates of protein tyrosine phosphatases. *Proc. Natl. Acad. Sci. USA* **94**, 1680-1685. doi:10.1073/pnas.94.5.1680

Frangioni, J. V., Beahm, P. H., Shifrin, V., Jost, C. A. and Neel, B. G. (1992). The nontransmembrane tyrosine phosphatase PTP-1B localizes to the endoplasmic reticulum via its 35 amino acid C-terminal sequence. *Cell* **68**, 545-560. doi:10.1016/0092-8674(92)90190-N

Fuentes, F. and Arregui, C. O. (2009). Microtubule and cell contact dependency of ER-bound PTP1B localization in growth cones. *Mol. Biol. Cell* **20**, 1878-1889. doi:10.1091/mbc.e08-07-0675

Gao, G., Prutzman, K. C., King, M. L., Scheswohl, D. M., DeRose, E. F., London, R. E., Schaller, M. D. and Campbell, S. L. (2004). NMR solution structure of the focal adhesion targeting domain of focal adhesion kinase in complex with a paxillin LD peptide: evidence for a two-site binding model. *J. Biol. Chem.* **279**, 8441-8451. doi:10.1074/jbc.M309808200

Giancotti, F. G. and Ruoslahti, E. (1999). Integrin Signaling. *Science* **285**, 1028-1033. doi:10.1126/science.285.5430.1028

Goñi, G. M., Epifano, C., Boskovic, J., Camacho-Artacho, M., Zhou, J., Bronowska, A., Martín, M. T., Eck, M. J., Kremer, L., Gräter, F. et al. (2014). Phosphatidylinositol 4,5-bisphosphate triggers activation of focal adhesion kinase by inducing clustering and conformational changes. *Proc. Natl. Acad. Sci. USA* **111**, E3177-E3186. doi:10.1073/pnas.1317022111

González Wusener, A. E., González, Á., Nakamura, F. and Arregui, C. O. (2016). PTP1B triggers integrin-mediated repression of myosin activity and modulates cell contractility. *Biology Open* **5**, 32-44. doi:10.1242/bio.015883

Guan, K. L. and Dixon, J. E. (1991). Evidence for protein-tyrosine-phosphatase catalysis proceeding via a cysteine-phosphate intermediate. *J. Biol. Chem.* **266**, 17026-17030. doi:10.1016/S0021-9258(19)47335-3

Guan, J.-L. and Shalloway, D. (1992). Regulation of focal adhesion-associated protein tyrosine kinase by both cellular adhesion and oncogenic transformation. *Nature* **358**, 690-692. doi:10.1038/358690a0

Haj, F. G., Verveer, P. J., Squire, A., Neel, B. G. and Bastiaens, P. I. H. (2002). Imaging sites of receptor dephosphorylation by PTP1B on the surface of the endoplasmic reticulum. *Science* **295**, 1708-1711. doi:10.1126/science.1067566

Hayashi, I., Vuori, K. and Liddington, R. C. (2002). The focal adhesion targeting (FAT) region of focal adhesion kinase is a four-helix bundle that binds paxillin. *Nat. Struct. Biol.* **9**, 101-106. doi:10.1038/nsb755

Hernández, M. V., Davies Sala, M. G., Balsamo, J., Lilien, J. and Arregui, C. O. (2006). ER-bound PTP1B is targeted to newly forming cell-matrix adhesions. *J. Cell Sci.* **119**, 1233-1243. doi:10.1242/jcs.02846

Hoellerer, M. K., Noble, M. E. M., Labesse, G., Campbell, I. D., Werner, J. M. and Arold, S. T. (2003). Molecular recognition of paxillin LD motifs by the focal adhesion targeting domain. *Structure* **11**, 1207-1217. doi:10.1016/j.str.2003.08.010

Horton, E. R., Humphries, J. D., Stutchbury, B., Jacquemet, G., Ballestrem, C., Barry, S. T. and Humphries, M. J. (2016). Modulation of FAK and Src adhesion signaling occurs independently of adhesion complex composition. *J. Cell Biol.* **212**, 349-364. doi:10.1083/jcb.201508080

Hubbard, S. R. (1997). Crystal structure of the activated insulin receptor tyrosine kinase in complex with peptide substrate and ATP analog. *EMBO J.* **16**, 5573-5581. doi:10.1093/emboj/16.18.5572

Huveneers, S. and Danen, E. H. J. (2009). Adhesion signaling - Crosstalk between integrins, Src and Rho. *J. Cell Sci.* **122**, 1059-1069. doi:10.1242/jcs.039446

Huyer, G., Liu, S., Kelly, J., Moffat, J., Payette, P., Kennedy, B., Tsaprailis, G., Gresser, M. J. and Ramachandran, C. (1997). Mechanism of inhibition of protein-tyrosine phosphatases by vanadate and pervanadate. *J. Biol. Chem.* **272**, 843-851. doi:10.1074/jbc.272.2.843

Ilić, D., Furuta, Y., Kanazawa, S., Takeda, N., Sobue, K., Nakatsuji, N., Nomura, S., Fujimoto, J., Fujimoto, J., Okada, M., et al. (1995). Reduced cell motility and enhanced focal adhesion contact formation in cells from FAK-deficient mice. *Nature* **377**, 539-544. doi:10.1038/377539a0

Irby, R. B. and Yeatman, T. J. (2000). Role of Src expression and activation in human cancer. *Oncogene* **19**, 5636-5642. doi:10.1038/sj.onc.1203912

Ishibe, S., Joly, D., Zhu, X. and Cantley, L. G. (2003). Phosphorylation-dependent paxillin-ERK association mediates hepatocyte growth factor-stimulated epithelial morphogenesis. *Mol. Cell* **12**, 1275-1285. doi:10.1016/S1097-2765(03)00406-4

Ishibe, S., Joly, D., Liu, Z.-X. and Cantley, L. G. (2004). Paxillin serves as an ERK-regulated scaffold for coordinating FAK and Rac activation in epithelial morphogenesis. *Mol. Cell* **16**, 257-267. doi:10.1016/j.molcel.2004.10.006

Jamieson, J. S., Tumbarello, D. A., Hallé, M., Brown, M. C., Tremblay, M. L. and Turner, C. E. (2005). Paxillin is essential for PTP-PEST-dependent regulation of cell spreading and motility: A role for paxillin kinase linker. *J. Cell Sci.* **118**, 5835-5847. doi:10.1242/jcs.02693

Jia, Z., Barford, D., Flint, A. J. and Tonks, N. K. (1995). Structural basis for phosphotyrosine peptide recognition by protein tyrosine phosphatase 1B. *Science* **268**, 1754-1758. doi:10.1126/science.7540771

Kadaré, G., Gervasi, N., Brami-Cherrier, K., Blockus, H., el Messari, S., Arold, S. T. and Girault, J.-A. (2015). Conformational dynamics of the focal adhesion targeting domain control specific functions of focal adhesion kinase in cells. *J. Biol. Chem.* **290**, 478-491. doi:10.1074/jbc.M114.593632

Kanchanawong, P., Shtengel, G., Pasapera, A. M., Ramko, E. B., Davidson, M. W., Hess, H. F. and Waterman, C. M. (2010). Nanoscale architecture of integrin-based cell adhesions. *Nature* **468**, 580-584. doi:10.1038/nature09621

Katz, B.-Z., Miyamoto, S., Teramoto, H., Zohar, M., Krylov, D., Vinson, C., Gutkind, J. S. and Yamada, K. M. (2002). Direct transmembrane clustering and cytoplasmic dimerization of focal adhesion kinase initiates its tyrosine phosphorylation. *Biochim. Biophys. Acta Mol. Cell Res.* **1592**, 141-152. doi:10.1016/S0167-4889(02)00308-7

Kholodenko, B. N., Hancock, J. F. and Kolch, W. (2010). Signalling ballet in space and time. *Nat. Rev. Mol. Cell Biol.* **11**, 414-426. doi:10.1038/nrm2901

Klemke, R. L., Cai, S., Giannini, A. L., Gallagher, P. J., de Lanerolle, P. and Cheresh, D. A. (1997). Regulation of cell motility by mitogen-activated protein kinase. *J. Cell Biol.* **137**, 481-492. doi:10.1083/jcb.137.2.481

Klinghoffer, R. A., Sachsenmaier, C., Cooper, J. A. and Soriano, P. (1999). Src family kinases are required for integrin but not PDGFR signal transduction. *EMBO J.* **18**, 2459-2471. doi:10.1093/emboj/18.9.2459

Kuo, M.-W., Wang, C.-H., Wu, H.-C., Chang, S.-J. and Chuang, Y.-J. (2011). Soluble THSD7A is an N-glycoprotein that promotes endothelial cell migration and tube formation in angiogenesis. *PLoS ONE* **6**, e29000. doi:10.1371/journal.pone.0029000

Lawson, C. D. and Burridge, K. (2014). The on-off relationship of Rho and Rac during integrin-mediated adhesion and cell migration. *Small GTPases* **5**, e27958. doi:10.4161/sgtp.27958

le Boeuf, F., Houle, F. and Huot, J. (2004). Regulation of vascular endothelial growth factor receptor 2-mediated phosphorylation of focal adhesion kinase by heat shock protein 90 and Src kinase activities. *J. Biol. Chem.* **279**, 39175-39185. doi:10.1074/jbc.M405493200

Lee, H. S., Cheerathodi, M., Chaki, S. P., Reyes, S. B., Zheng, Y., Lu, Z., Paidassi, H., DerMardirossian, C., Lacy-Hulbert, A., Rivera, G. M. et al. (2015). Protein tyrosine phosphatase-PEST and β8 integrin regulate spatiotemporal patterns of RhoGDI1 activation in migrating cells. *Mol. Cell. Biol.* **35**, 1401-1413. doi:10.1128/MCB.00112-15

Liang, F., Lee, S.-Y., Liang, J., Lawrence, D. S. and Zhang, Z.-Y. (2005). The role of protein-tyrosine phosphatase 1B in integrin signaling. *J. Biol. Chem.* **280**, 24857-24863. doi:10.1074/jbc.M502780200

Lietha, D., Cai, X., Ceccarelli, D. F. J., Li, Y., Schaller, M. D. and Eck, M. J. (2007). Structural basis for the autoinhibition of focal adhesion kinase. *Cell* **129**, 1177-1187. doi:10.1016/j.cell.2007.05.041

Lim, Y., Han, I., Jeon, J., Park, H., Bahk, Y.-Y. and Oh, E.-S. (2004). Phosphorylation of focal adhesion kinase at tyrosine 861 is crucial for ras transformation of fibroblasts. *J. Biol. Chem.* **279**, 29060-29065. doi:10.1074/jbc.M401183200

Lim, Y., Lim, S.-T., Tomar, A., Gardel, M., Bernard-Trifilo, J. A., Xiao, L. C., Uryu, S. A., Canete-Soler, R., Zhai, J., Lin, H. et al. (2008). PyK2 and FAK connections to p190Rho guanine nucleotide exchange factor regulate RhoA activity, focal adhesion formation, and cell motility. *J. Cell Biol.* **180**, 187-203. doi:10.1083/jcb.200708194

Lipfert, L., Haimovich, B., Schaller, M. D., Cobb, B. S., Parsons, J. T. and Brugge, J. S. (1992). Integrin-dependent phosphorylation and activation of the protein tyrosine kinase pp125(FAK) in platelets. *J. Cell Biol.* **119**, 905-912. doi:10.1083/jcb.119.4.905

Liu, F., Hill, D. E. and Chernoff, J. (1996). Direct binding of the proline-rich region of protein tyrosine phosphatase 1B to the Src homology 3 domain of p130(Cas). *J. Biol. Chem.* **271**, 31290-31295. doi:10.1074/jbc.271.49.31290

Liu, F., Sells, M. A. and Chernoff, J. (1998). Protein tyrosine phosphatase 1B negatively regulates integrin signaling. *Curr. Biol.* **8**, 173-176. doi:10.1016/S0960-9822(98)70066-1

Liu, G., Guibao, C. D. and Zheng, J. (2002). Structural insight into the mechanisms of targeting and signaling of focal adhesion kinase. *Mol. Cell. Biol.* **22**, 2751-2760. doi:10.1128/MCB.22.8.2751-2760.2002

Maier, J. A., Martinez, C., Kasavajhala, K., Wickstrom, L., Hauser, K. E. and Simmerling, C. (2015). ff14SB: improving the accuracy of protein side chain and backbone parameters from ff99SB. *J. Chem. Theory Computat.* **11**, 3696-3713. doi:10.1021/acs.jctc.5b00255

Martínez, P. T., Navajas, P. L. and Lietha, D. (2020). FAK structure and regulation by membrane interactions and force in focal adhesions. *Biomolecules* **10**, 179. doi:10.3390/biom10020179

Miranti, C. K. and Brugge, J. S. (2002). Sensing the environment: a historical perspective on integrin signal transduction. *Nat. Cell Biol.* **4**, E83-E90. doi:10.1038/ncb0402-e83

Mitra, S. K. and Schlaepfer, D. D. (2006). Integrin-regulated FAK-Src signaling in normal and cancer cells. *Curr. Opin. Cell Biol.* **18**, 516-523. doi:10.1016/j.ceb.2006.08.011

Monteleone, M. C., González Wusener, A. E., Burdisso, J. E., Conde, C., Cáceres, A. and Arregui, C. O. (2012). ER-bound protein tyrosine phosphatase PTP1B interacts with Src at the plasma membrane/substrate interface. *PLoS ONE* **7**, e38948. doi:10.1371/journal.pone.0038948

Mukherjee, A., Singh, R., Udayan, S., Biswas, S., Reddy, P. P., Manmadhan, S., George, G., Kumar, S., Das, R., Rao, B. M. et al. (2020). A fyn biosensor reveals pulsatile, spatially localized kinase activity and signaling crosstalk in live mammalian cells. *eLife* **9**, e50571. doi:10.7554/eLife.50571

Nader, G. P. F., Ezratty, E. J. and Gundersen, G. G. (2016). FAK, talin and PIPKI 3 regulate endocytosed integrin activation to polarize focal adhesion assembly. *Nat. Cell Biol.* **18**, 491-503. doi:10.1038/ncb3333

Nakamura, K., Yano, H., Schaefer, E. and Sabe, H. (2001). Different modes and qualities of tyrosine phosphorylation of Fak and Pyk2 during epithelial-mesenchymal transdifferentiation and cell migration: Analysis of specific phosphorylation events using site-directed antibodies. *Oncogene* **20**, 2626-2635. doi:10.1038/sj.onc.1204359

Ng, D. H. J., Humphries, J. D., Byron, A., Millon-Frémillon, A. and Humphries, M. J. (2014). Microtubule-dependent modulation of adhesion complex composition. *PLoS ONE* **9**, e115213. doi:10.1371/journal.pone.0115213

Niediek, V., Born, S., Hampe, N., Kirchgeßner, N., Merkel, R. and Hoffmann, B. (2012). Cyclic stretch induces reorientation of cells in a Src family kinase- and p130Cas-dependent manner. *Eur. J. Cell Biol.* **91**, 118-128. doi:10.1016/j.ejcb.2011.10.003

Oneyama, C. and Okada, M. (2015). MicroRNAs as the fine-tuners of Src oncogenic signalling. *J. Biochem.* **157**, 431-438. doi:10.1093/jb/mvv036

Pasapera, A. M., Schneider, I. C., Rericha, E., Schlaepfer, D. D. and Waterman, C. M. (2010). Myosin II activity regulates vinculin recruitment to focal adhesions through FAK-mediated paxillin phosphorylation. *J. Cell Biol.* **188**, 877-890. doi:10.1083/jcb.200906012

Petit, V., Boyer, B., Lentz, D., Turner, C. E., Thiery, J. P. and Vallés, A. M. (2000). Phosphorylation of tyrosine residues 31 and 118 on paxillin regulates cell migration through an association with CRK in NBT-II cells. *J. Cell Biol.* **148**, 957-970. doi:10.1083/jcb.148.5.957

Pradhan, S., Alrehani, N., Patel, V., Khatlani, T. and Vijayan, K. V. (2010). Cross-talk between serine/threonine protein phosphatase 2A and protein tyrosine phosphatase 1B regulates Src activation and adhesion of integrin αIIbβ3to fibrinogen. *J. Biol. Chem.* **285**, 29059-29068. doi:10.1074/jbc.M109.085167

Prutzman, K. C., Gao, G., King, M. L., Iyer, V. V., Mueller, G. A., Schaller, M. D. and Campbell, S. L. (2004). The focal adhesion targeting domain of focal adhesion kinase contains a hinge region that modulates tyrosine 926 phosphorylation. *Structure* **12**, 881-891. doi:10.1016/j.str.2004.02.028

Pullara, F., Asciutto, E. K. and General, I. J. (2017). Mechanisms of Activation and Subunit Release in Ca2+/Calmodulin-Dependent Protein Kinase II. *J. Phys. Chem. B* **121**, 10344-10352. doi:10.1021/acs.jpcb.7b09214

Rahuel, J., Gay, B., Erdmann, D., Strauss, A., García-Echeverría, C., Furet, P., Caravatti, G., Fretz, H., Schoepfer, J. and Grütter, M. G. (1996). Structural basis for specificity of GRB2-SH2 revealed by a novel ligand binding mode. *Nat. Struct. Biol.* **3**, 586-589. doi:10.1038/nsb0796-586

Ren, Y., Meng, S., Mei, L., Zhao, Z. J., Jove, R. and Wu, J. (2004). Roles of Gab1 and SHP2 in Paxillin tyrosine dephosphorylation and Src activation in response to epidermal growth factor. *J. Biol. Chem.* **279**, 8497-8505. doi:10.1074/jbc.M312575200

Renshaw, M. W., Price, L. S. and Schwartz, M. A. (1999). Focal adhesion kinase mediates the integrin signaling requirement for growth factor activation of MAP kinase. *J. Cell Biol.* **147**, 611-618. doi:10.1083/jcb.147.3.611

Richardson, A. and Parsons, J. T. (1996). A mechanism for regulation of the adhesion-associated protein tyrosine kinase pp125FAK. *Nature* **380**, 538-540. doi:10.1038/380538a0

Ringer, P., Colo, G., Fässler, R. and Grashoff, C. (2017). Sensing the mechano-chemical properties of the extracellular matrix. *Matrix Biol.* **64**, 6-16. doi:10.1016/j.matbio.2017.03.004

Ripamonti, M., Liaudet, N., Azizi, L., Bouvard, D., Hytönen, V. P. and Wehrle-Haller, B. (2021). Structural and functional analysis of LIM domain-dependent recruitment of paxillin to αvβ3 integrin-positive focal adhesions. *Commun. Biol.* **4**, 380. doi:10.1038/s42003-021-01886-9

Robertson, J., Jacquemet, G., Byron, A., Jones, M. C., Warwood, S., Selley, J. N., Knight, D., Humphries, J. D. and Humphries, M. J. (2015). Defining the phospho-adhesome through the phosphoproteomic analysis of integrin signalling. *Nat. Commun.* **6**, 6265. doi:10.1038/ncomms7265

Ruest, P. J., Shyamali, R., Ergang, S., Mernaugh, R. L. and Hanks, S. K. (2000). Phosphospecific antibodies reveal focal adhesion kinase activation loop phosphorylation in nascent and mature focal adhesions and requirement for the autophosphorylation site. *Cell Growth Differ.* **11**, 41-48.

Salmeen, A., Andersen, J. N., Myers, M. P., Tonks, N. K. and Barford, D. (2000). Molecular basis for the dephosphorylation of the activation segment of the insulin receptor by protein tyrosine phosphatase 1B. *Mol. Cell* **6**, 1401-1412. doi:10.1016/S1097-2765(00)00137-4

Sastry, S. K., Lyons, P. D., Schaller, M. D. and Burridge, K. (2002). PTP-PEST controls motility through regulation of Rac1. *J. Cell Sci.* **115**, 4305-4316. doi:10.1242/jcs.00105

Schaller, M. D. (2010). Cellular functions of FAK kinases: Insight into molecular mechanisms and novel functions. *J. Cell Sci.* **123**, 1007-1013. doi:10.1242/jcs.045112

Schaller, M. D. and Parsons, J. T. (1995). pp125FAK-dependent tyrosine phosphorylation of paxillin creates a high-affinity binding site for Crk. *Mol. Cell. Biol.* **15**, 2635-2645. doi:10.1128/MCB.15.5.2635

Schaller, M. D. and Schaefer, E. M. (2001). Multiple stimuli induce tyrosine phosphorylation of the Crk-binding sites of paxillin. *Biochem. J.* **360**, 57-66. doi:10.1042/bj3600057

Schaller, M. D., Hildebrand, J. D., Shannon, J. D., Fox, J. W., Vines, R. R. and Parsons, J. T. (1994). Autophosphorylation of the focal adhesion kinase, pp125FAK, directs SH2-dependent binding of pp60src. *Mol. Cell. Biol.* **14**, 1680-1688.

Schaller, M. D., Hildebrand, J. D. and Parsons, J. T. (1999). Complex formation with focal adhesion kinase: A mechanism to regulate activity and subcellular

localization of Src kinases. *Mol. Biol. Cell* **10**, 3489-3505. doi:10.1091/mbc.10.10.3489

Schlaepfer, D. D. and Hunter, T. (1996a). Evidence for in vivo phosphorylation of the Grb2 SH2-domain binding site on focal adhesion kinase by Src-family protein-tyrosine kinases. *Mol. Cell. Biol.* **16**, 5623-5633. doi:10.1128/MCB.16.10.5623

Schlaepfer, D. D. and Hunter, T. (1996b). Signal transduction from the extracellular matrix - a role for the focal adhesion protein-tyrosine kinase FAK. *Cell Struct. Funct.* **21**, 445-450. doi:10.1247/csf.21.445

Schlaepfer, D. D. and Hunter, T. (1997). Focal adhesion kinase overexpression enhances Ras-dependent integrin signaling to ERK2/mitogen-activated protein kinase through interactions with and activation of c-Src. *J. Biol. Chem.* **272**, 13189-13195. doi:10.1074/jbc.272.20.13189

Schlaepfer, D. D., Hanks, S. K., Hunter, T. and van der Geer, P. (1994). Integrin-mediated signal transduction linked to Ras pathway by GRB2 binding to focal adhesion kinase. *Nature* **372**, 786-791. doi:10.1038/372786a0

Schlaepfer, D. D., Hauck, C. R. and Sieg, D. J. (1999). Signaling through focal adhesion kinase. *Prog. Biophys. Mol. Biol.* **71**, 435-478. doi:10.1016/S0079-6107(98)00052-2

Schneider, I. C., Hays, C. K. and Waterman, C. M. (2009). Epidermal growth factor-induced contraction regulates paxillin phosphorylation to temporally separate traction generation from de-adhesion. *Mol. Biol. Cell* **20**, 3155-3167. doi:10.1091/mbc.e09-03-0219

Shen, Y., Lyons, P., Cooley, M., Davidson, D., Veillette, A., Salgia, R., Griffin, J. D. and Schaller, M. D. (2000). The noncatalytic domain of protein-tyrosine phosphatase-PEST targets paxillin for dephosphorylation in vivo. *J. Biol. Chem.* **275**, 1405-1413. doi:10.1074/jbc.275.2.1405

Sparta, B., Pargett, M., Minguet, M., Distor, K., Bell, G. and Albeck, J. G. (2015). Receptor level mechanisms are required for epidermal growth factor (EGF)-stimulated extracellular signal-regulated kinase (ERK) activity pulses. *J. Biol. Chem.* **290**, 24784-24792. doi:10.1074/jbc.M115.662247

Sternberg, S. R. (1983). Biomedical image processing. *Computer* **16**, 22-34. doi:10.1109/MC.1983.1654163

Takino, T., Tamura, M., Miyamori, H., Araki, M., Matsumoto, K., Sato, H. and Yamada, K. M. (2003). Tyrosine phosphorylation of the CrkII adaptor protein modulates cell migration. *J. Cell Sci.* **116**, 3145-3155. doi:10.1242/jcs.00632

Theodosiou, M., Widmaier, M., Böttcher, R. T., Rognoni, E., Veelders, M., Bharadwaj, M., Lambacher, A., Austen, K., Müller, D. J., Zent, R. et al. (2016). Kindlin-2 cooperates with talin to activate integrins and induces cell spreading by directly binding paxillin. *eLife* **5**, e10130. doi:10.7554/eLife.10130

Thomas, J. W., Cooley, M. A., Broome, J. M., Salgia, R., Griffin, J. D., Lombardo, C. R. and Schaller, M. D. (1999). The role of focal adhesion kinase binding in the regulation of tyrosine phosphorylation of paxillin. *J. Biol. Chem.* **274**, 36684-36692. doi:10.1074/jbc.274.51.36684

Tilghman, R. W., Slack-Davis, J. K., Sergina, N., Martin, K. H., Iwanicki, M., Hershey, E. D., Beggs, H. E., Reichardt, L. F. and Parsons, J. T. (2005). Focal adhesion kinase is required for the spatial organization of the leading edge in migrating cells. *J. Cell Sci.* **118**, 2613-2623. doi:10.1242/jcs.02380

Tsubouchi, A., Sakakura, J., Yagi, R., Mazaki, Y., Schaefer, E., Yano, H. and Sabe, H. (2002). Localized suppression of RhoA activity by Tyr31/118-phosphorylated paxillin in cell adhesion and migration. *J. Cell Biol.* **159**, 673-683. doi:10.1083/jcb.200202117

Volberg, T., Romer, L., Zamir, E. and Geiger, B. (2001). pp60(c-src) and related tyrosine kinases: a role in the assembly and reorganization of matrix adhesions. *J. Cell Sci.* **114**, 2279-2289. doi:10.1242/jcs.114.12.2279

Walkiewicz, K. W., Girault, J.-A. and Arold, S. T. (2015). How to awaken your nanomachines: Site-specific activation of focal adhesion kinases through ligand interactions. *Prog. Biophys. Mol. Biol.* **119**, 60-71. doi:10.1016/j.pbiomolbio.2015.06.001

Waterman-Storer, C. M. and Salmon, E. D. (1998). Endoplasmic reticulum membrane tubules are distributed by microtubules in living cells using three distinct mechanisms. *Curr. Biol.* **8**, 798-807. doi:10.1016/S0960-9822(98)70321-5

Wheeler, D. L., Iida, M. and Dunn, E. F. (2009). The Role of Src in Solid Tumors. *Oncologist* **14**, 667-678. doi:10.1634/theoncologist.2009-0009

Xie, Y., Wang, J., Zhang, Y., Liu, X., Wang, X., Liu, K., Huang, X. and Wang, Y. (2016). Quantitative profiling of spreading-coupled protein tyrosine phosphorylation in migratory cells. *Sci. Rep.* **6**, 31811. doi:10.1038/srep31811

Zaidel-Bar, R. and Geiger, B. (2010). The switchable integrin adhesome. *J. Cell Sci.* **123**, 1385-1388. doi:10.1242/jcs.066183

Zaidel-Bar, R., Milo, R., Kam, Z. and Geiger, B. (2007). A paxillin tyrosine phosphorylation switch regulates the assembly and form of cell-matrix adhesions. *J. Cell Sci.* **120**, 137-148. doi:10.1242/jcs.03314

Zamir, E., Katz, B. Z., Aota, S. I., Yamada, K. M., Geiger, B. and Kam, Z. (1999). Molecular diversity of cell-matrix adhesions. *J. Cell Sci.* **112**, 1655-1669. doi:10.1242/jcs.112.11.1655

Zhang, S. Q., Yang, W., Kontaridis, M. I., Bivona, T. G., Wen, G., Araki, T., Luo, J., Thompson, J. A., Schraven, B. L., Philips, M. R. et al. (2004a). Shp2 regulates Src family kinase activity and Ras/Erk activation by controlling Csk recruitment. *Mol. Cell* **13**, 341-355. doi:10.1016/S1097-2765(04)00050-4

Zhang, Z., Izaguirre, G., Lin, S.-Y., Lee, H. Y., Schaefer, E. and Haimovich, B. (2004b). The phosphorylation of vinculin on tyrosine residues 100 and 1065, mediated by Src kinases, affects cell spreading. *Mol. Biol. Cell* **15**, 4234-4247. doi:10.1091/mbc.e04-03-0264

Zhang, Z., Lin, S.-Y., Neel, B. G. and Haimovich, B. (2006). Phosphorylated α-actinin and protein-tyrosine phosphatase 1B coregulate the disassembly of the focal adhesion kinase·Src complex and promote cell migration. *J. Biol. Chem.* **281**, 1746-1754. doi:10.1074/jbc.M509590200

Zhang, X., Tee, Y. H., Heng, J. K., Zhu, Y., Hu, X., Margadant, F., Ballestrem, C., Bershadsky, A., Griffiths, G. and Yu, H. (2010). Kinectin-mediated endoplasmic reticulum dynamics supports focal adhesion growth in the cellular lamella. *J. Cell Sci.* **123**, 3901-3912. doi:10.1242/jcs.069153

Zheng, Y., Xia, Y., Hawke, D., Halle, M., Tremblay, M. L., Gao, X., Zhou, X. Z., Aldape, K., Cobb, M. H., Xie, K. et al. (2009). FAK phosphorylation by ERK primes Ras-induced tyrosine dephosphorylation of FAK mediated by PIN1 and PTP-PEST. *Mol. Cell* **35**, 11-25. doi:10.1016/j.molcel.2009.06.013

Zhou, Z., Feng, H. and Bai, Y. (2006). Detection of a hidden folding intermediate in the focal adhesion target domain: Implications for its function and folding. *Proteins: Structure, Function and Bioinformatics* **65**, 259-265. doi:10.1002/prot.21107

Zhu, L., Liu, H., Lu, F., Yang, J., Byzova, T. V. and Qin, J. (2019). Structural basis of paxillin recruitment by kindlin-2 in regulating cell adhesion. *Structure* **27**, 1686-1697. doi:10.1016/j.str.2019.09.006

FIGURE S1

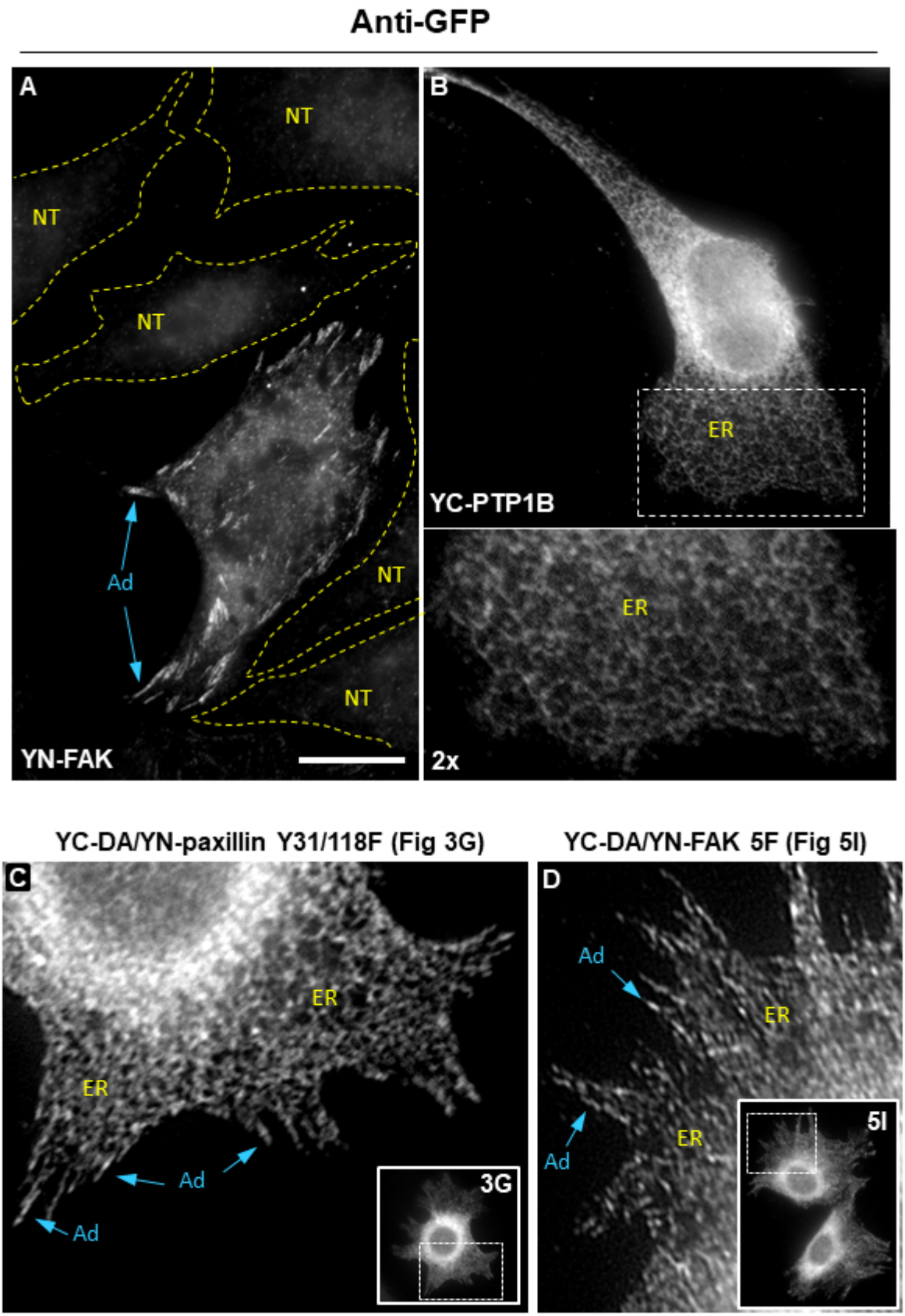

Fig. S1. Recognition of BiFC constructs with anti-GFP.

PTP1B WT cells transfected with YN-FAK (A) or YC-PTP1B (B) and stained with the polyclonal anti-GFP. Note that the signal distribution agrees with the expected localization of each construct, YN-FAK in adhesions (Ad, arrows in A) and YC-PTP1B in the ER (ER label and inset in B). Note the dim and diffuse background signal in non transfected cells (delimited by the yellow dashed lines and labeled NT). In cells co-transfected with BiFC pairs targeted to the ER and adhesion compartments, their co-expression can be recognized by the different signal distribution (C and D). The panels C and D are 4x magnifications of cells shown in Fig. 3G and Fig. 5I (added at bottom) and correspond to the BiFC analysis of PTP1B DA with paxillin Y31/118F (Fig. 3G) and YN-FAK 5F (Fig. 5I), respectively. In these mutants the BiFC signal is negative, but the anti-GFP labeling confirms the co-expression of both BiFC constructs, as revealed by the simultaneous distribution of adhesions (Ad) and ER in panels C and D. Scale bar, 20 µm.

FIGURE S2

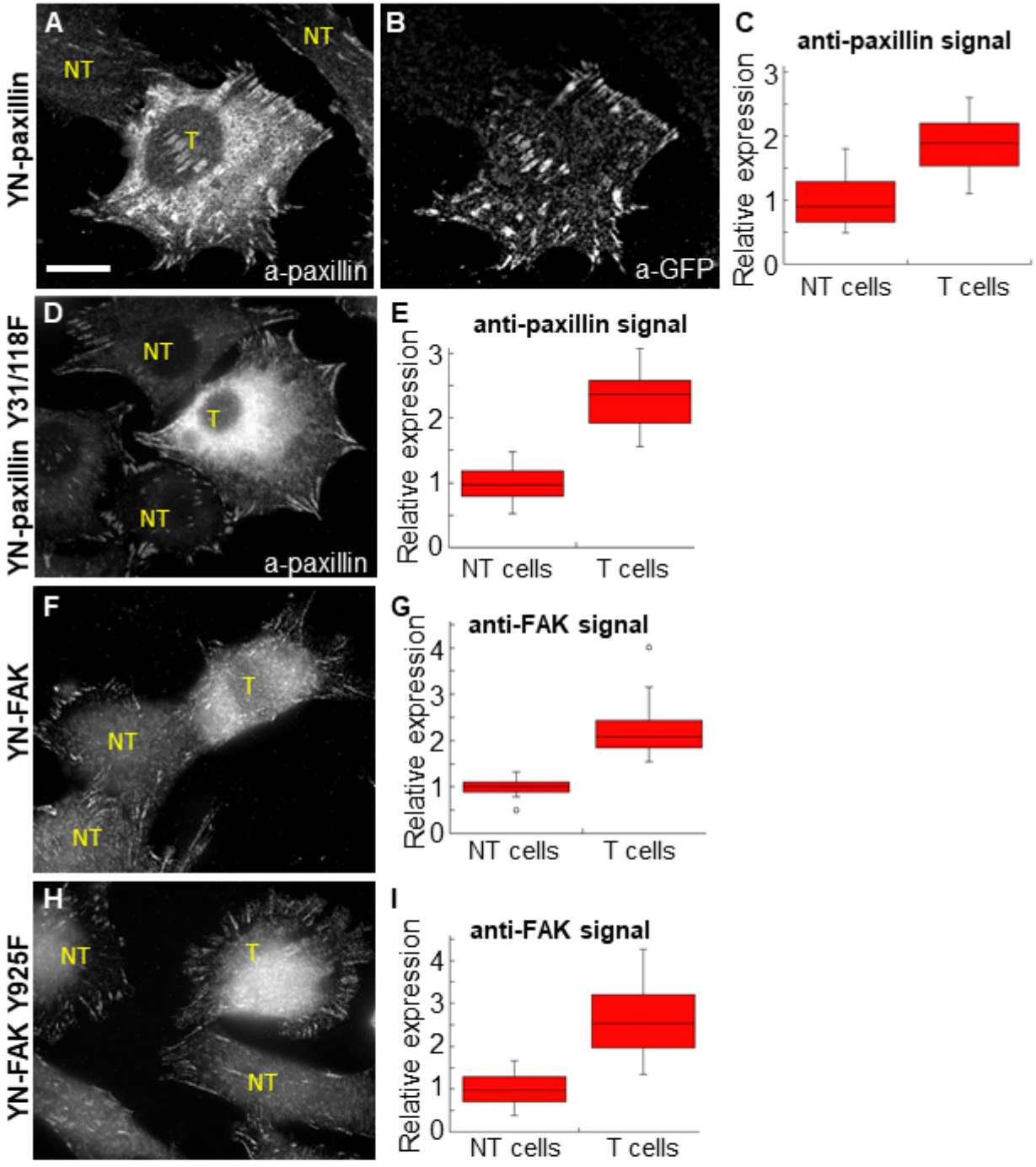

Fig. S2. Distribution and expression levels of BiFC constructs. PTP1B WT cells transfected with YN-paxillin (A-C), YN-paxillin Y31/118F (D,E), YN-FAK (F,G), and YN-FAK Y925F (H,I) were stained with anti-paxillin (A,C-E), anti-GFP (B), and anti-FAK (F-I), and analyzed by wide-field fluorescence microscopy. Transfected (T) and non-transfected (NT) cells were indicated. Box plots show the quantification of mean intensity in non-transfected (endogenous levels) and transfected (endogenous plus exogenous levels) cells. Values were normalized to the mean of NT cells. Boxes enclose 50% of the data with the median value displayed as a line. The top and bottom of the box mark the limits of the lower and upper quartiles. The lines extending from the top and bottom of each box mark the minimum and maximum values in the data set within 1.5*IQD (Inter Quartile Distance) from the lower and upper quartiles, respectively. YN-paxillin, n=27; YN-paxillin Y31/118F, n=26; YN-FAK, n=21; YN-FAK Y925F, n=21. Note that the signal average in transfected cells doubles that in non-transfected cells. Scale bar, 20 μm.

FIGURE S3

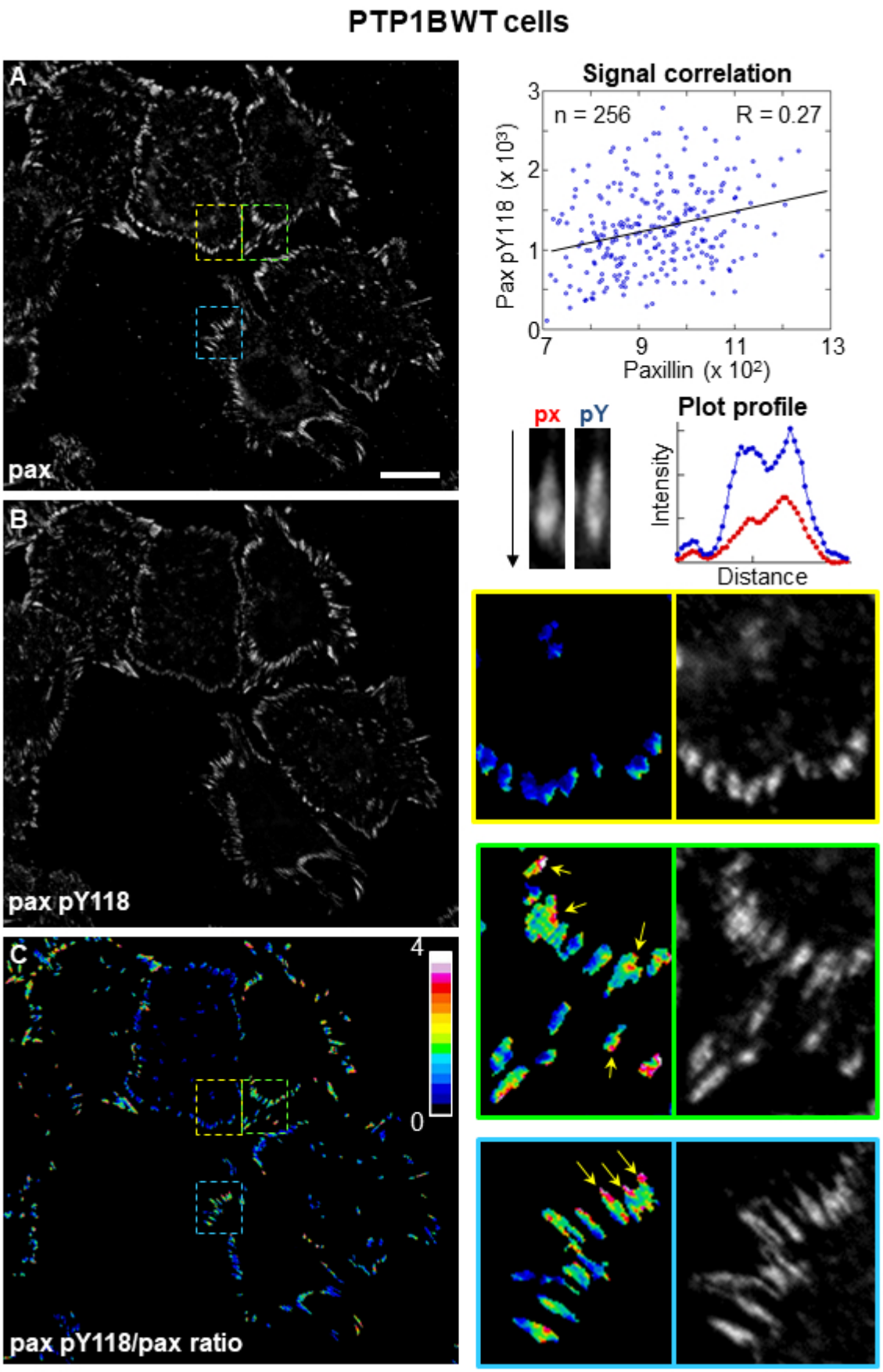

Fig. S3. Phosphorylation level of paxillin in adhesions of PTP1B WT cells. Cells plated on fibronectin were fixed and double stained with a monoclonal anti-total paxillin (pax, A) and a polyclonal anti-phospho-paxillin (pax pY118, B) followed by fluorescent secondary antibodies. Cells were observed by wide-field fluorescence microscopy. Images were processed as indicated in Materials and Methods. The distribution of phosphorylated to total paxillin was assessed by ratio imaging (C). Enlargements of peripheral regions were shown for three different cells (dashed boxes in A,C). Arrows point hotspots of phospho-paxillin within adhesions. The graph displays the average signal of pax pY118 and pax in 256 adhesions of five cells (blue dots) in the field. The Pearson's correlation coefficient R reveals low correlation between both signals. The pax pY118 signal shows high variability (range min/max 115-2792) compared to the pax signal (range min/max 709-1281). The variation of each signal within a single adhesion is shown in the plot profile. The arrow indicates the origin and end of the linescan. Scale bar, 20 µm.

FIGURE S4

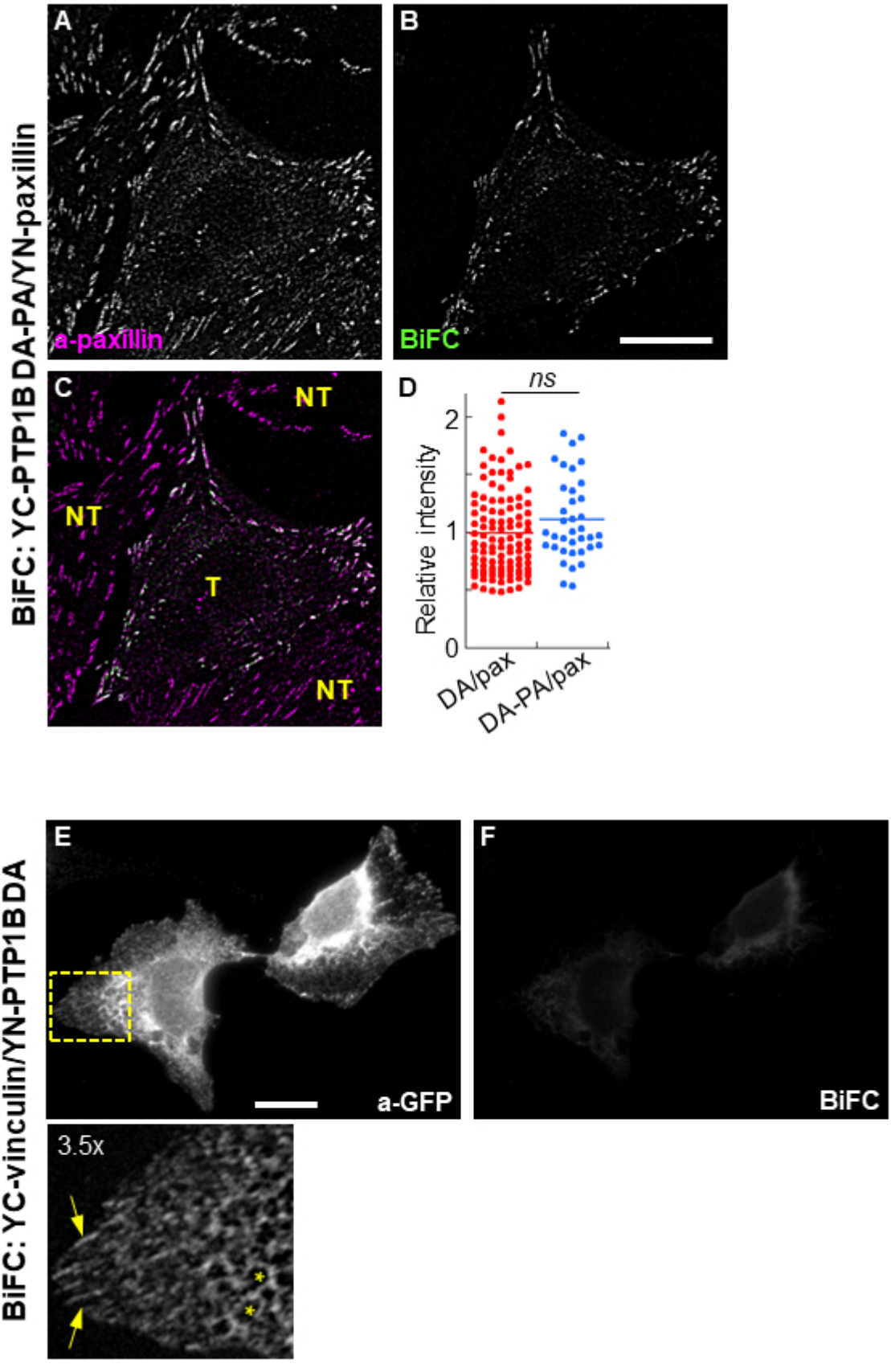

Fig. S4. BiFC analysis of YN-paxillin/YC-PTP1B DA-PA and YC-vinculin/YN-PTP1B DA pairs. PTP1B WT cells were co-transfected with the YN-paxillin/YC-PTP1B DA-PA BiFC pair (A-D) and analyzed by confocal microscopy. Representative images labeled with anti-paxillin (A), displaying BiFC (B), and the merge image (C). T and NT indicate transfected and non-transfected cells, respectively. Quantification of the relative intensity of BiFC to GFP signal (not shown) in peripheral cell-matrix adhesions (D). Ratios were normalized to the mean of DA/pax ratio. DA/pax, n=109; DA-PA/pax, n=37. The mean value is displayed as a line. DA/pax was compared to DA-PA/pax using the Mann-Whitney non-parametric test. *ns* (not significant). PTP1B WT cells were co-transfected with the YC-vinculin/YN-PTP1B DA BiFC pair (E,F) and analyzed by wide field microscopy. Two representative co-transfected cells were stained with anti-GFP and visualized in the red channel (E). They show the combined distribution of both BiFC constructs, YN-PTP1B DA in the ER, and YC-vinculin in peripheral adhesions (yellow asterisks and yellow arrows in the 4.5x magnification, respectively). (F) The same field shown in (E) but visualized in the BiFC channel. Note the lack of BiFC signal. Scale bar, 20 µm.

FIGURE S5

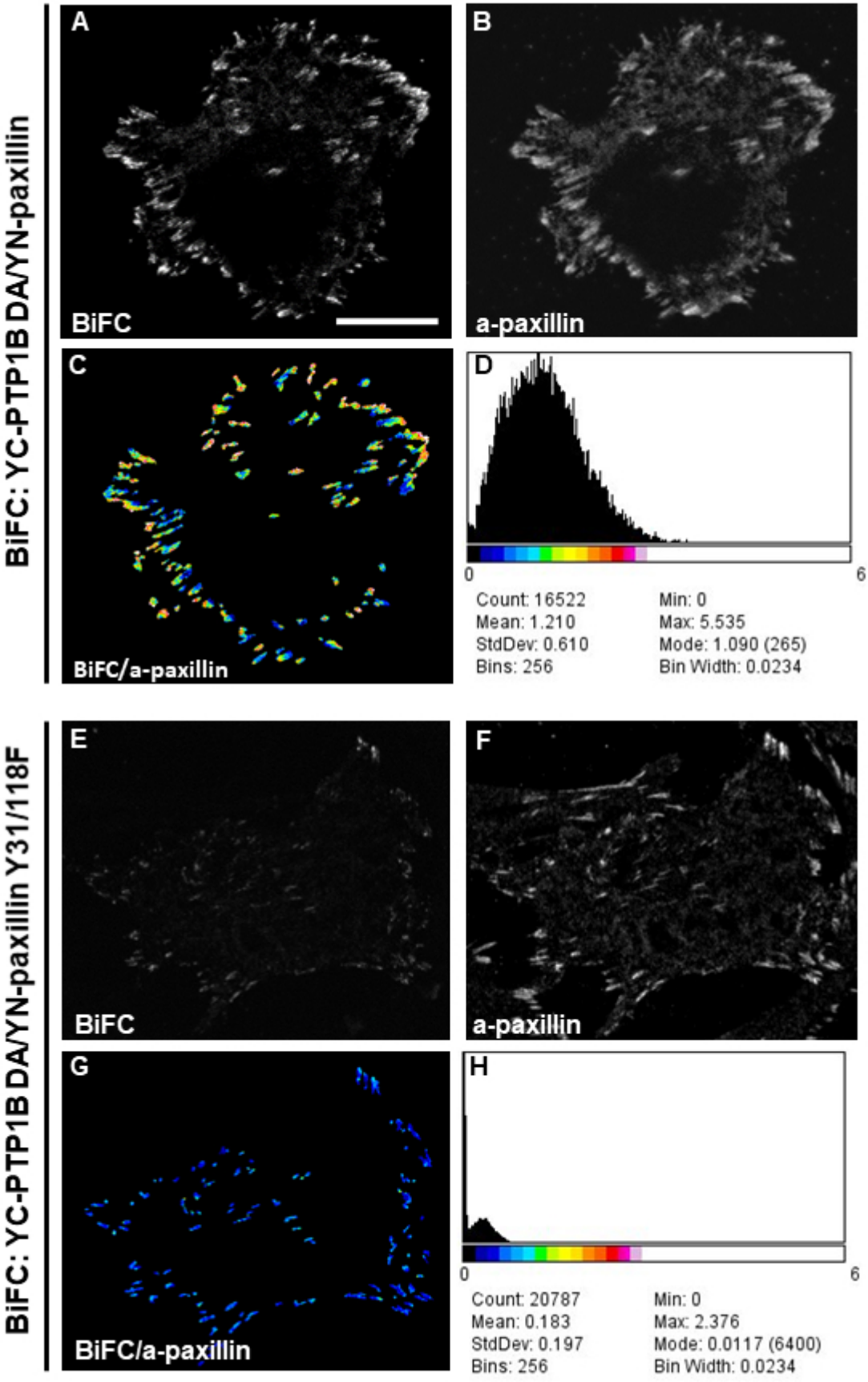

Fig. S5. Analysis of BiFC/anti-paxillin ratio in adhesions. Representative PTP1B WT cells co-expressing YC-PTP1B DA/YN-paxillin (A-C), and YC-PTP1B DA/YN-paxillin Y31/118F (E-G). Cells immunolabeled with anti-paxillin show similar paxillin expression (B,F). However, the positive BiFC signal in cells co-expressing the YC-PTP1B DA/YN-paxillin pair (A) is significantly reduced in cells co-expressing the YC-PTP1B DA/YN-paxillin Y31/118F pair (E). This is better appreciated in the BiFC/anti-paxillin ratios within segmented adhesions (C,G). Ratios are represented by a 16-color palette between a 0-3 range. Histograms representing the frequency distribution of the mean intensity of BiFC/a-paxillin ratios (D, H). The total pixel count as well as the mean, modal, minimum and maximum values are shown. Scale bar, 20 μm.

FIGURE S6

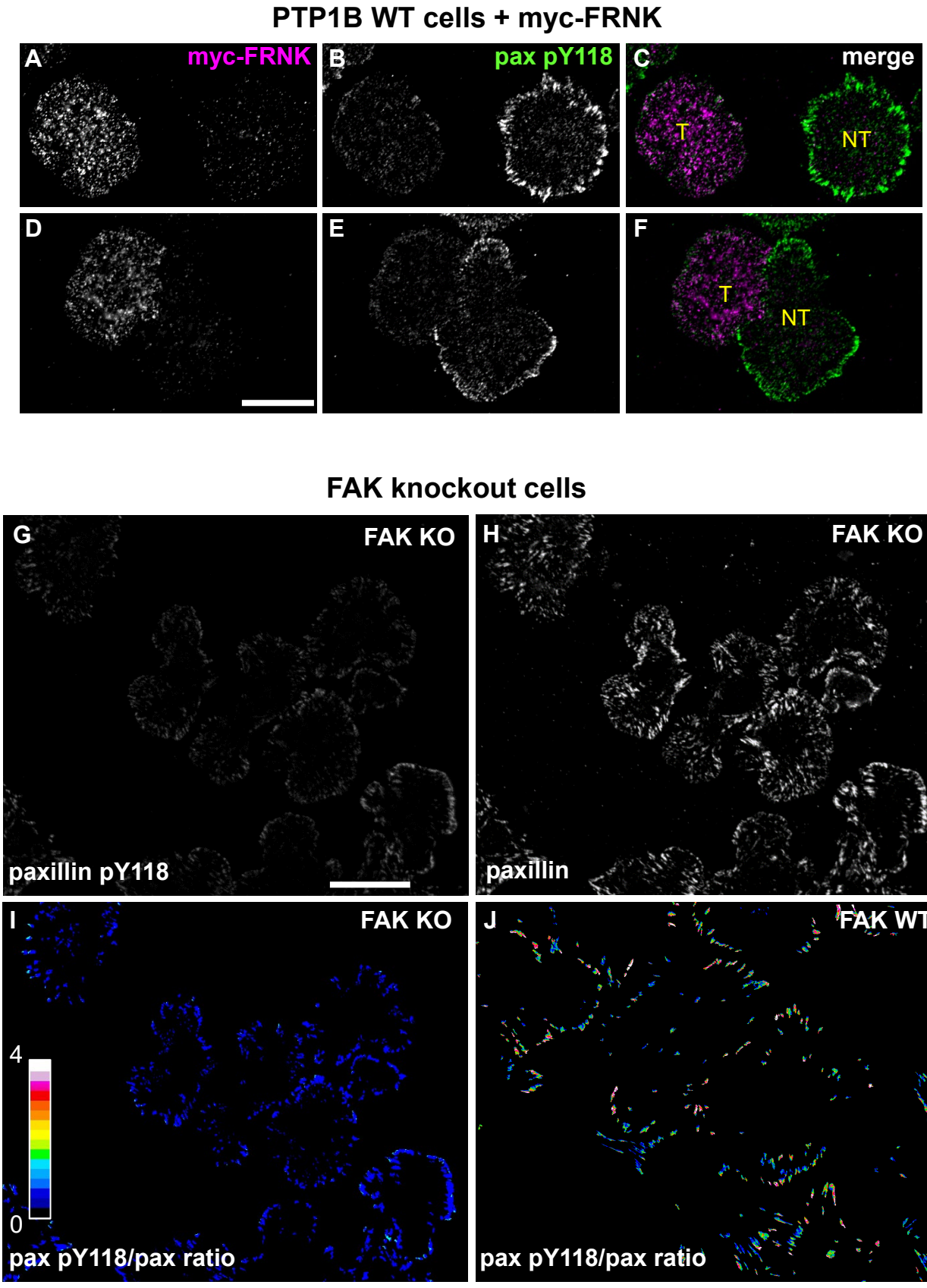

Fig. S6. Phosphorylation level of paxillin in adhesions of cells with impaired FAK function. PTP1B cells transfected with a dominant negative construct of FAK, myc-FRNK (A-F), were plated on fibronectin to form adhesions, and then fixed and double stained with a monoclonal anti-myc (A,D) and a polyclonal anti-phospho-paxillin (pax pY118, B,E) followed by fluorescent secondary antibodies. Cells were observed by wide-field fluorescence microscopy (two representative examples were shown). In merge images (C,F) note that transfected (T) cells show reduced phospho-paxillin signal compared to non-transfected (NT) cells. FAK knockout cells (G-J) co-expressing YN-paxillin and YC-PTP1B DA were plated on fibronectin to form adhesions, and then fixed and double stained with a polyclonal anti-phospho-paxillin (pax pY118, G) and monoclonal anti-paxillin (H), followed by fluorescent secondary antibodies. Cells were observed by wide-field fluorescence microscopy. Note that although paxillin organizes in peripheral adhesions of FAK KO cells, the level of phosphorylation is barely detected. This is better appreciated in BiFC/anti-paxillin ratios within segmented adhesions (I). Images were processed as indicated in Materials and Methods. For comparison, a BiFC/anti-paxillin ratio image from FAK WT cells was shown (J). Scale bar, 20 μm.

FIGURE S7

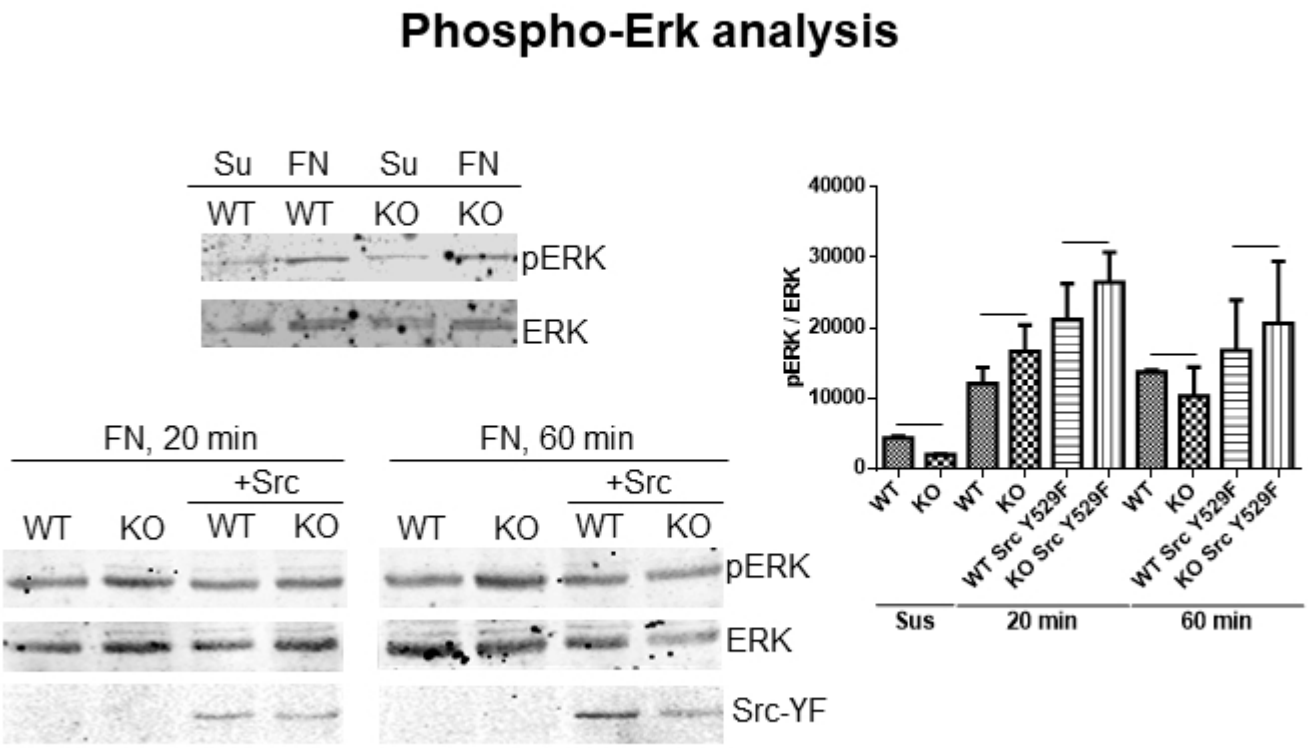

Fig. S7. Assessment of Erk activity. Western blots of serum-starved PTP1B knockout (KO) cells and KO cells reconstituted with wild type PTP1B (WT). The upper panel shows a comparison between cells kept 30 min in suspension and cells plated on fibronectin (10µg/ml) for 20 min. Lower panels show the results of cells non-transfected and transfected with constitutive active Src Y529F-HA plated 20 and 60 min on fibronectin coated dishes. Specific antibodies were used for detection of pERK, ERK, and Src Y529F-HA. Three independent experiments were used for quantification using ImageJ software. Normalized pERK/ERK values, according to LI-COR published protocol, were used for the relative comparison of the different conditions. Bars represent means ± S.E.M. Statistical analysis for normalized pERK/ERK, comparing WT vs KO in each condition, was determined using one-way ANOVA, followed by the Bonferroni´s multiple comparison post hoc test. There was not a significant difference between the means of the indicated pairs.

J. Cell Sci. doi:10.1242/jcs.258769: Supplementary information

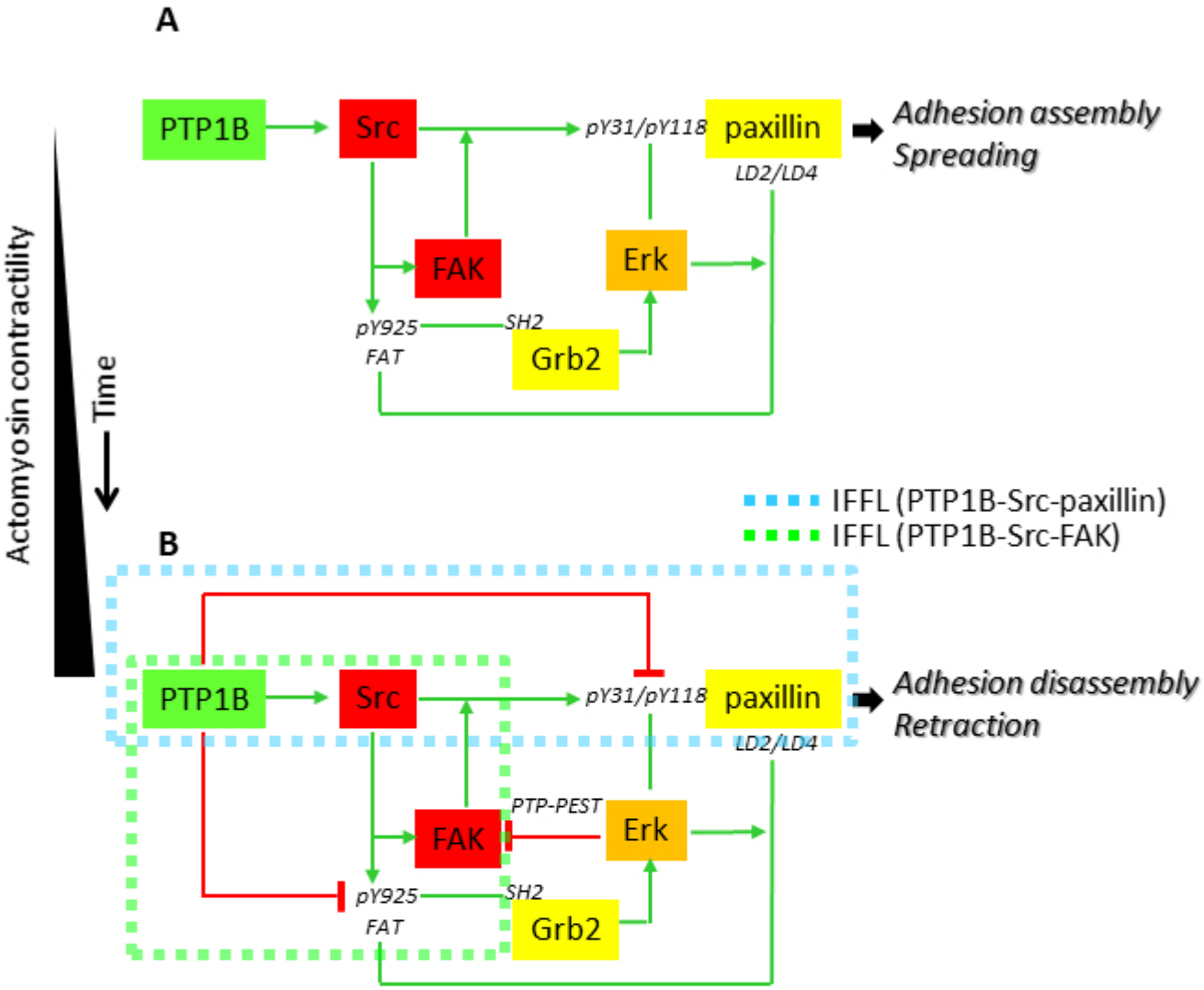

Fig. S8. Model of PTP1B regulation mediated by FAK and paxillin. PTP1B is an upstream activator of Src, which phosphorylates and activates FAK. Both Src and FAK phosphorylate paxillin, leading to adhesion assembly and spreading. In turn, phosphorylation of FAK FAT domain at Y925, recruits Grb2, and promotes Erk activation (A). With a time-delay, PTP1B dephosphorylates FAK and paxillin, leading to adhesion disassembly and lamellar retraction. PTP1B regulation configurates incoherent feedforward loops (IFFLs) that tunes paxillin (dashed blue box) and FAK (dashed green box) outputs depending on their phosphorylation states (B).

Table S1. Conservation of charged amino acids in regions of helices 1, 2 and 4, close to Y925. The *Conservation* column refers to the specific amino acid conservation, while the *Charge conservation* column refers to conservation of the charge type (positive or negative). In bold face, very high conservation values.

Amino acid	Conservation (%)	Charge conservation (%)	
Y925	96		
D922	97	**100**	Helix 1
K923	39	48	
E926	25	38	
R962	96	**98**	
D969	42	63	Helix 2
E970	96	**99**	
K1032	100	**100**	
D1036	100	**100**	Helix 4
D1039	98	**98**	
R1042	99	**100**	